THE JOURNAL OF BIOLOGICAL CHEMISTRY VOL. 284, NO. 9, pp. 5557–5573, February 27, 2009

Ribosomal S6 Kinase 2 Directly Phosphorylates the 5-Hydroxytryptamine 2A (5-HT_{2A}) Serotonin Receptor, Thereby Modulating 5-HT_{2A} Signaling*

Received for publication, July 24, 2008, and in revised form, November 18, 2008 Published, JBC Papers in Press, December 22, 2008, DOI 10.1074/jbc.M805705200

Ryan T. Strachan[‡], Douglas J. Sheffler[§], Belinda Willard[¶], Michael Kinter[¶], Janna G. Kiselar[‖], and Bryan L. Roth[‡1]**

*From the [‡]Department of Biochemistry, Case Western Reserve University Medical School, Cleveland, Ohio 44106, the **Department of Pharmacology, University of North Carolina Medical School, Chapel Hill, North Carolina 27599, the [§]Department of Pharmacology, Vanderbilt University, Nashville, Tennessee 37232, [¶]Cell Biology, Cleveland Clinic Lerner Research Institute, Cleveland, Ohio 44195, and the [‖]Case Western Reserve University Center for Proteomics, Cleveland, Ohio 44106*

The 5-hydroxytryptamine 2A (5-HT_{2A}) receptor is a member of the G protein-coupled receptor superfamily (GPCR) and plays a key role in transducing a variety of cellular signals elicited by 5-hydroxytryptamine in both peripheral and central tissues. Despite its broad physiological importance, our current understanding of 5-HT_{2A} receptor regulation is incomplete. We recently reported the novel finding that the multifunctional ERK effector ribosomal S6 kinase 2 (RSK2) physically interacts with the 5-HT_{2A} receptor third intracellular (i3) loop and modulates receptor signaling (Sheffler, D. J., Kroeze, W. K., Garcia, B. G., Deutch, A. Y., Hufeisen, S. J., Leahy, P., Bruning, J. C., and Roth, B. L. (2006) *Proc. Natl. Acad. Sci. U. S. A.* 103, 4717–4722). We report here that RSK2 directly phosphorylates the 5-HT_{2A} receptor i3 loop at the conserved residue Ser-314, thereby modulating 5-HT_{2A} receptor signaling. Furthermore, these studies led to the discovery that RSK2 is required for epidermal growth factor-mediated heterologous desensitization of the 5-HT_{2A} receptor. We arrived at these conclusions via multiple lines of evidence, including *in vitro* kinase experiments, tandem mass spectrometry, and site-directed mutagenesis. Our findings were further validated using phospho-specific Western blot analysis, metabolic labeling studies, and whole-cell signaling experiments. These results support a novel regulatory mechanism in which a downstream effector of the ERK/MAPK pathway directly interacts with, phosphorylates, and modulates signaling of the 5-HT_{2A} serotonin receptor. To our knowledge, these findings are the first to demonstrate that a downstream member of the ERK/MAPK cascade phosphorylates a GPCR as well as mediates cross-talk between a growth factor and a GPCR.

The 5-HT_{2A}[2] receptor plays a key role in transducing a variety of cellular signals elicited by 5-HT in both peripheral and central tissues (75). These include the following: 1) platelet aggregation (1); 2) vascular and nonvascular smooth muscle contraction (2); 3) cognitive processes underlying working memory (3); 4) modulating sensory processing in the cortex (4); and 5) mediating the actions of most, but not all, hallucinogens that act as 5-HT_{2A} receptor agonists (5, 6). Moreover, dysregulation of the 5-HT_{2A} receptor has been linked to the etiology of several psychiatric disorders, including depression, anxiety, and schizophrenia, thus highlighting the importance of gaining a more thorough understanding of the precise regulation of 5-HT_{2A} receptors (7).

The 5-HT_{2A} receptor belongs to the GPCR superfamily that encompasses molecular targets for an extreme diversity of endogenous and exogenous ligands that are essential for nearly every physiological process (8). Extensive studies focusing on the G protein-coupled receptor kinase-arrestin pathway and the second messenger-dependent protein kinase (cAMP-dependent protein kinase and protein kinase C (PKC)) pathways suggest that direct GPCR phosphorylation remains the predominant mechanism for rapidly attenuating the signaling of many GPCRs (9, 10). Additional kinases have also been shown to phosphorylate GPCRs, and it is likely that many yet to be discovered kinases regulate GPCR signaling (11).

Several studies have demonstrated that PKC modulates 5-HT_{2A} receptor signaling *in vivo* and *in vitro*. Our early studies (12) showed that activation of PKC by phorbol dibutyrate inhibited 5-HT_{2A}-mediated signaling. Many subsequent studies in a variety of cellular contexts have replicated these observations (13–18). In addition to PKC, recent reports suggest that calmodulin-dependent protein kinase II and G protein-coupled receptor kinase 2/3 regulate 5-HT_{2A} signaling (18, 19), although the role of G protein-coupled receptor kinases is cell-specific (20). From these prior studies it is clear that selected kinases modulate 5-HT_{2A} receptor function, although the site(s) of action and their mechanisms remain unknown.

* This work was supported, in whole or in part, by National Institutes of Health Grants RO1MH61887, NO1MH32004, and U19MH82441 (to B. L. R.). The costs of publication of this article were defrayed in part by the payment of page charges. This article must therefore be hereby marked "*advertisement*" in accordance with 18 U.S.C. Section 1734 solely to indicate this fact.

[1] To whom correspondence should be addressed: Dept. of Pharmacology, 4009 Genetics Medicine CB 7365, Chapel Hill, NC 27599-7365. Fax: 919-843-5788; E-mail: bryan_roth@med.unc.edu.

[2] The abbreviations used are: 5-HT_{2A}, serotonin 2A receptor; 5-HT, serotonin; GPCR, G protein-coupled receptor; RSK2, ribosomal S6 kinase 2; ERK/MAPK, extracellular signal-regulated kinase/mitogen-activated protein kinase; RTK, receptor tyrosine kinase; EGF, epidermal growth factor; GFP, green fluorescent protein; MS, mass spectrometry; IP, inositol phosphate; DOI, (±)-2,5-dimethoxy-4-iodoamphetamine hydrochloride; α-Me5-HT, α-methyl serotonin; RFU, relative fluorescence unit; CID, collision-induced dissociation; FLIPR, fluorometric imaging plate reader; BSA, bovine serum albumin; DMEM, Dulbecco's modified Eagle's medium; Ni-NTA, nickel-nitrilotriacetic acid; Ab, antibody; MOPS, 4-morpholinepropanesulfonic acid; CHAPS, 3-[(3-cholamidopropyl)dimethylammonio]-1-propanesulfonic acid; PKC, protein kinase C; EEDQ, *N*-ethoxycarbonyl-2-ethoxy-1,2-dihydroquinoline; IP_3, inositol 1,4,5-trisphosphate.

Recently we discovered that RSK2, a downstream effector of the ERK/MAPK pathway, regulates the signaling of several GPCRs, including 5-HT$_{2A}$, P2Y-purinergic, PAR-1-thrombinergic, β_1-adrenergic receptor, and bradykinin-B receptors (21). RSK2 is a well characterized member of the RSK family of multifunctional ERK effectors (RSK1–4), and RSK2 has been shown to phosphorylate a wide variety of cytoplasmic and nuclear proteins (22). We (21) recently showed that RSK2 interacts with the 5-HT$_{2A}$ i3 loop within a conserved region containing an RSK2-like consensus phosphorylation motif (^{275}RAKLAS^{280}) (23). Importantly, RSK2 modulated 5-HT$_{2A}$ receptor signaling independent of changes in 5-HT$_{2A}$ receptor subcellular distribution, global G protein function, and without altering the expression of any genes known to be involved in serotonergic signal transduction. Our findings implied that RSK2 acts proximal to receptor activation, at the level of receptor-G protein coupling, perhaps via direct phosphorylation of 5-HT$_{2A}$ receptors.

Here we provide multiple lines of evidence demonstrating that activated RSK2 phosphorylates the 5-HT$_{2A}$ receptor i3 loop at the conserved residue Ser-314. We show that mutation of Ser-314 renders the 5-HT$_{2A}$ receptor insensitive to RSK2 regulation, thereby resulting in increased signaling mirroring observations in RSK2$^{-/-}$ fibroblasts (21). To our knowledge this is the first report that a downstream member of the ERK/MAPK cascade phosphorylates a GPCR. Moreover, these studies uncovered a novel regulatory mechanism whereby RSK2 is required for EGF-mediated heterologous desensitization of the 5-HT$_{2A}$ receptor. These data support the intriguing notion that 5-HT$_{2A}$ receptor responsiveness in cells is influenced by receptor tyrosine kinase (RTK) activation.

Because null mutations of RSK2 lead to Coffin-Lowry syndrome, which is characterized by mental retardation, cardiovascular disorders, and a schizophrenia-like psychosis (24), these findings may explain, in part, some of the clinical manifestations of this syndrome.

EXPERIMENTAL PROCEDURES

Materials—Cell culture reagents were supplied by Invitrogen and Cambrex (East Rutherford, NJ). Human embryonic kidney (HEK) 293T cells were purchased from the American Type Culture Collection (Manassas, VA), and the RSK2$^{+/+}$ and RSK2$^{-/-}$ mouse embryonic fibroblasts were generated as described previously (25). Serotonin (5-HT), (±)-2,5-dimethoxy-4-iodoamphetamine hydrochloride (DOI), α-methyl serotonin (α-Me5-HT), M2 FLAG affinity resin, FLAG peptide, rabbit polyclonal anti-FLAG antibody, human EGF, and all standard reagents were supplied by Sigma. *N*-Ethoxycarbonyl-2-ethoxy-1,2-dihydroquinoline (EEDQ) was supplied by Acros Organics (Morris Plains, NJ). SL0101 was supplied by Toronto Research Chemicals, Inc. (Ontario, Canada), and BI-D1870 was supplied by the Division of Signal Transduction Therapy, University of Dundee (Scotland, UK). Primers for molecular biology were synthesized by Invitrogen, and restriction endonucleases were supplied by New England Biolabs (Ipswich, MA). [^{3}H]Ketanserin (67.0 Ci/mmol), [^{3}H]myoinositol (21.7 Ci/mmol), [γ-^{32}P]ATP (3000 Ci/mmol), and $^{32}P_i$ (orthophosphate, 285.6 Ci/mg) were obtained from PerkinElmer Life Sciences). The polyclonal rabbit GFP antibody was obtained from Abcam (Cambridge, UK). The rabbit polyclonal phospho-p90 RSK (Ser(P)-386) antibody was from Cell Signaling Technology, Inc. (Danvers, MA). The rabbit polyclonal $G\alpha_q$, goat polyclonal and mouse monoclonal anti-RSK2 antibodies, and protein A/G PLUS beads were from Santa Cruz Biotechnology (Santa Cruz, CA). The horseradish peroxidase-conjugated goat anti-rabbit and horse anti-goat secondary antibodies were from Vector Laboratories (Burlingame, CA).

Cell Culture and Transfection—HEK 293T and mouse embryonic fibroblast cells were maintained in Dulbecco's modified Eagle's medium (DMEM) supplemented with 10% fetal bovine serum, 1 mM sodium pyruvate, 100 units/ml penicillin, and 100 μg/ml streptomycin. Cells were grown at 37 °C in a humidified environment in the presence of 5% CO_2. FuGENE (Roche Applied Science) was used exactly as described by the manufacturer to transiently transfect subconfluent HEK 293T cells cultured in 10-cm dishes. Cells were used within 72 h of transfection.

RSK2 Constructs—The native mouse RSK2 cDNA was subcloned from pMT2-HA-RSK2 (26) into pcDNA3 (Invitrogen) and pEGFP-C1 (Clontech) introducing 5′HindIII and 3′KpnI sites using the following primers: AAAA**AAGCTT**TAGCCACCATGCCGCTGGCGCAGCTG (HindIII in boldface type) and ACCTCAACAGCCCTGTGA**GGTACC**TTTT (KpnI in boldface type). For virus production the RSK2 sequence was subsequently modified by site-directed mutagenesis to remove an internal EcoRI site and subcloned into the pBABE retroviral vector containing a puromycin resistance gene (pBABEpuro) (27). The primers were as follows: AAAA**GAATTC**GCCACCAGCCGCTGGCG (EcoRI in boldface type) and AAAA**GTCGAC**TCACAGGGCTGTTGAGGTG (SalI in boldface type). Kinase-dead RSK2 mutants in pcDNA3 and pEGFP-C1 were generated as outlined below.

Affinity-tagged 5-HT$_{2A}$ Receptor Construction—The 5-HT$_{2A}$ receptor containing an N-terminal *Hemophilus influenzae* hemagglutinin membrane insertion signal sequence and contiguous FLAG and hexahistidine affinity tags (FLAG-His$_6$ 5-HT$_{2A}$) was constructed using the rat FLAG 5-HT$_{2A}$ receptor (28) as a template for overlap extension PCR. Briefly, two amplicons inserting 5′ EcoRI (amplicon 1) and 3′ SalI (amplicon 2) restriction sites as well as an overlapping hexahistidine affinity tag sequence were generated. Amplicon 1 was generated with the following primers: AAA**GAATTC**GCCACCATGAAGACGATCAT (EcoRI in boldface type) and GAT**GTGATGATGATGATGATG**CTTATCGTCGTCATCCTTG (hexahistidine sequence in boldface type). Amplicon 2 was generated with the following primers: **CATCATCATCATCATCA-C**ATCGAGGGCCGCG (hexahistidine sequence in boldface type) and AAA**GTCGAC**TCACACACAGCTAACCTTTTCATTC (SalI in boldface type). The amplicons were annealed and extended to produce the full-length FLAG-His$_6$ 5-HT$_{2A}$ product. The FLAG-His$_6$ 5-HT$_{2A}$ cDNA was subcloned into the pBABEpuro retroviral vector for stable line generation using the EcoRI and SalI amplicon primers. The phosphorylation-deficient mutant (S314A) in pBABEpuro was mutagenized as outlined below. The FLAG-His$_6$ 5-HT$_{2A}$ receptor insert in pBABEpuro was subcloned into pcDNA3 for receptor purifica-

tion using the following primers: AAA**AAGCTT**ACCACCATGAAGAC (HindIII in boldface type) and AAA**TCTAGA**TCACACACAGCTAACCTTTTCATTC (XbaI highlighted). Each FLAG-His$_6$ 5-HT$_{2A}$ receptor construct was confirmed by automated sequencing (Genome Analysis Facility, University of North Carolina, Chapel Hill) and alignment of the overlapping sequences in Vector NTi (Invitrogen).

Construction and Tandem Affinity Purification of I3 Loop Peptides—The i3 loop peptide (amino acids 252–328 of the rat 5-HT$_{2A}$ receptor) was purified similarly to a previous report (29). This purification scheme yielded a final 79-amino acid peptide (8772 Da) containing an extra N-terminal Met and extra C-terminal Gly. Briefly, the i3 loop peptide was subcloned (introducing 5′ NdeI and 3′ NheI) into the inducible pET11a expression vector (Novagen, Madison, WI) as a fusion protein located N-terminal to an inducible protein splicing element (intein) attached to a modified chitin binding domain containing a C-terminal hexahistidine affinity tag (IMPACT, New England Biolabs, Inc.). Phosphorylation-deficient mutants were constructed as outlined below. BL21(DE3)pLysS *Escherichia coli* (Stratagene, La Jolla, CA) were freshly transformed with i3 loop peptide constructs in pET11a, grown to $A_{600\ nm} = 0.6$ in LB medium containing 60 μg/ml ampicillin and 34 μg/ml chloramphenicol, and induced with 0.5 mM isopropyl 1-thio-β-D-galactopyranoside for 5 h at 25 °C. The *E. coli* were collected, washed, and frozen at −20 °C. The frozen pellets were resuspended in cold lysis buffer (20 mM HEPES, 500 mM NaCl, 0.1% Triton X-100, and 100 μM phenylmethylsulfonyl fluoride, pH 8.0) and passed three times through a French press at 1500 p.s.i., and the supernatant was isolated by centrifugation at 12,000 × *g* for 45 min. The supernatant was loaded onto a Ni-NTA column (Qiagen Inc., Valencia, CA), washed with 7-bed volumes of wash buffer (20 mM HEPES, 500 mM NaCl, and 20 mM imidazole, pH 8.0), and the fusion protein recovered with 3 bed volumes of elution buffer (20 mM HEPES, 500 mM NaCl, and 250 mM imidazole, pH 8.0). Fractions containing the 60-kDa fusion protein, as determined by Western blot analysis, were pooled and applied to a chitin column (New England Biolabs, Inc., Ipswich, MA). The chitin column was washed with 7 bed volumes of wash buffer (20 mM HEPES, 1 M NaCl, pH 8.0) and incubated for 16 h at 4 °C with intein cleavage buffer (20 mM HEPES, 1 M NaCl, 50 mM dithiothreitol, pH 8.0). The i3 loop peptide was recovered with 3 bed volumes of elution buffer (20 mM HEPES, 500 mM NaCl, pH 8.0), and each fraction was analyzed by Western blot. Fractions containing the liberated i3 loop peptide (apparent molecular mass of 6 kDa) were combined and further purified and concentrated using 30- and 3-kDa Centricon filter units (Millipore, Billerica, MA), respectively. Protein concentrations were determined by the Bradford method (30), and peptides were frozen at −80 °C until further use.

Site-directed Mutagenesis—The QuikChange site-directed mutagenesis kit (Stratagene) was used to generate kinase-dead RSK2 mutants, i3 loop peptide mutants, and a full-length FLAG-His$_6$ 5-HT$_{2A}$ receptor mutant using the wild-type constructs as PCR templates. The following primers were used to generate kinase-dead RSK2 mutants (mutated codon in boldface type): 1) K100A, GCTAGACAGCTTTATGCCATG**GCA**GTATTAAAGAAGGCCAC and GTGGCCTTCTTTAATAC**TGC**CATGGCATAAAGCTGTCTAGC; 2) K451A, CAAACATGGAGTTTGCCGTG**GCG**ATTATTGATAAAAGCAAGAGAG and CTCTCTTGCTTTTATCAATAAT**CGC**CACGGCAAACTCCATGTTTG. The S280A i3 loop peptide mutant in pET11a was generated using mutagenesis primers ACTCGAGCCAAACTAGCC**GCC**TTCAGCTTCCTCCCTCAG and CTGAGGGAGGAAGCTGAA**GGC**GGCTAGTTTGGCTCGAGT. The phosphorylation-deficient S314A i3 loop peptide and receptor mutants were both generated using the mutagenesis primers GGCCGAAGGACGATGCAG**GCC**ATCAGCAATGAGCAAAAG and CTTTTGCTCATTGCTGAT**GGC**CTGCATCGTCCTTCGGCC. All constructs were confirmed by automated sequencing (Genomics Core Facility, Cleveland, OH, and Genome Analysis Facility, University of North Carolina, Chapel Hill) and alignment of the overlapping sequences in Vector NTi (Invitrogen).

Retrovirus Production and 5-HT$_{2A}$ Polyclonal Stable Line Generation—Amphotropic retrovirus was produced from helper virus-free HEK 293 (HEK 293TS) host cells using the pBABEpuro retroviral vector and pCL10A1 amphotropic packaging plasmid (Imgenex, San Diego). Briefly, HEK 293TS cells were co-transfected with 3 μg of RSK2 or receptor cDNA and 3 μg of pCL10A1. Viral supernatants were collected 24–36 h post-transfection, combined with Polybrene (8 μg/ml), and added to RSK2$^{-/-}$ and RSK2$^{+/+}$ mouse embryonic fibroblasts previously used to identify RSK2 as a modulator of 5-HT$_{2A}$ receptor signaling (21). Polyclonal cell populations were selected with puromycin (3–4 μg/ml) 48 h after infection. Polyclonal populations of fibroblasts expressing wild-type 5-HT$_{2A}$ and 5-HT$_{2A}$-S314A receptors were expanded and characterized for receptor expression using radioligand binding as described previously (20). The Ligand program (31) was used to calculate affinity (K_d) and receptor density (B_{max}) values from homologous competition curves (see "Results"). For IP time course and EGF desensitization studies, we used previously generated RSK2$^{+/+}$ and RSK2$^{-/-}$ fibroblasts stably expressing similar amounts of 5-HT$_{2A}$ receptors (21).

Affinity Purification of Epitope-tagged 5-HT$_{2A}$ Receptors and RSK2—For *in vitro* kinase assays HEK 293T cells were transfected with 10 μg of FLAG-His$_6$ 5-HT$_{2A}$ cDNA and harvested 48 h post-transfection in cold phosphate-buffered saline. The cell pellets were solubilized with cold lysis buffer A (50 mM HEPES, 150 mM NaCl, 1 mM EDTA, 1.0% CHAPS, and EDTA-free protease inhibitor mixture, pH 7.5) at a concentration of 10 ml/g cell pellet for 20 min at 4 °C. The cleared supernatant was added to EZ-view M2 FLAG affinity resin and rocked for 2 h at 4 °C. The M2 FLAG resin was washed twice with 10 volumes of lysis buffer A and once with 10 volumes of lysis buffer B (50 mM HEPES, 150 mM NaCl, 1.0% CHAPS, EDTA-free protease inhibitors, pH 7.5). The receptors were eluted from the M2 FLAG resin with 200 μM 1× FLAG peptide, supplemented to 10 mM imidazole, and added to Ni-NTA resin. The Ni-NTA resin was incubated for 2 h at 4 °C with gentle agitation and washed four times with 10 volumes of wash buffer (lysis buffer B + 20 mM imidazole, pH 7.5). The FLAG-His$_6$ 5-HT$_{2A}$ receptor was eluted from the Ni-NTA resin with elution buffer (lysis buffer B + 250 mM imidazole, pH 7.5) and stored at −80 °C. For co-

immunoprecipitation experiments, HEK-293 cells were transiently co-transfected with FLAG-5-HT$_{2A}$ and cyan fluorescent protein, FLAG-5-HT$_{2A}$ and RSK2-GFP, FLAG-5-HT$_{2A}$ and RSK2-K100A-GFP, or FLAG-5-HT$_{2A}$ and RSK2-K451A-GFP cDNA. Immunoprecipitations were performed as described previously (28). Immunoprecipitation of RSK2 and detection of Ser(P)-386 was performed following 18 h of serum starvation as described previously (32).

Immunoblotting and Antibody Generation—Purified i3 loop peptides and 5-HT$_{2A}$ receptors were immunoblotted using standard procedures (20), except for phospho-specific immunoblots that were blocked with 3% bovine serum albumin (BSA). Specifically, i3 loop peptides were resolved on 4–20% gradient SDS-polyacrylamide gels and immunoblotted with the i3 loop antibody (antibody 1A, 1:3000) targeting amino acids 280–295 of the rat 5-HT$_{2A}$ receptor (29). 5-HT$_{2A}$ receptors were resolved on 10% SDS-polyacrylamide gels and immunoblotted with the FLAG antibody (1:1000), an antibody directed against the rat 5-HT$_{2A}$ C terminus (5-HT$_{2A}$-CT Ab, 1:1000), or the phospho-Ser-314-specific antibody (Ser(P)-314 Ab, 1:2000). The C-terminal Ab was generated similarly as indicated in a previous report (33). Briefly, two New Zealand White rabbits were immunized with the synthetic peptide ^{428}QKKNSQEDAEQTVDDC^{443} conjugated to BSA in Freund's complete adjuvant (Invitrogen). Bleeds were screened for selectivity using concentrated rat 5-HT$_{2A}$ and 5-HT$_{2C}$ receptors. Serum from the first extension bleed selectively detected the 5-HT$_{2A}$ receptor, which was blocked by preincubation with the antigenic peptide. The Ser(P)-314 Ab was generated against a synthetic phosphopeptide ^{307}AGRRTMQS(PO$_3$)ISNEQKAC^{322} (Biomer Technology, Hayward, CA). Two New Zealand White rabbits were immunized with the phosphopeptide conjugated to keyhole limpet hemocyanin in Freund's complete adjuvant, and bleeds were characterized against both the unmodified peptide and the phosphopeptide. Serum from the second bleed selectively detected <10 ng of the phosphopeptide. RSK2 (1:1000) was detected as described previously (21). Immunoreactive bands were quantified using Kodak Imaging software (Eastman Kodak Co., New Haven, CT).

In Vitro Kinase Assays—*In vitro* kinase assays included the following: 1) purified, activated RSK2 (Upstate-Millipore, Billerica, MA) diluted in enzyme buffer (20 mM MOPS, 1 mM EGTA, 0.01% Brij-35, 5% glycerol, 0.1% 2-mercaptoethanol, 1 mg/ml BSA, pH 7.5); 2) i3 loop peptide or FLAG-His$_6$ 5-HT$_{2A}$ receptor substrates; and 3) [γ-^{32}P]ATP or unlabeled ATP diluted in assay buffer (75 mM $MgCl_2$, 20 mM MOPS, 25 mM β-glycerol phosphate, 5 mM EGTA, 1 mM sodium orthovanadate, 1 mM dithiothreitol, pH 7.2). We assayed for [^{32}P]phosphate incorporation by incubating purified i3 loop peptide or purified FLAG-His$_6$ 5-HT$_{2A}$ receptor with 0.4–0.8 ng/μl RSK2 in the presence of 0.4–0.04 μCi/μl [γ-^{32}P]ATP for 1 h at 30 °C. The reactions were terminated by heating the samples for 5 min at 65 °C in SDS sample buffer and resolved on a 4–20% gradient (Invitrogen) or 10% SDS-polyacrylamide gels. The gels were dried and imaged on a Storm 840 PhosphorImager and analyzed using ImageQuant software (Amersham Biosciences). Kinetic measurements were performed under initial velocity conditions determined from a pilot experiment showing linear incorporation of [^{32}P]phosphate into the i3 loop peptide over 30 min using 0.4 ng/μl RSK2. Briefly, seven concentrations (2.3–140 μM) of i3 loop peptide were incubated with RSK2 in the presence of 10 μM unlabeled ATP and 0.04 μCi/μl [γ-^{32}P]ATP (7000 cpm/pmol ATP). The reactions were terminated by heating the samples for 5 min at 65 °C in SDS sample buffer and resolved on a 4–20% gradient SDS-polyacrylamide gel. Radioactivity was quantified by liquid scintillation counting and analyzed by nonlinear regression to determine V_{max} and K_m (GraphPad, San Diego). For the mass spectrometry and phospho-specific antibody approaches, we incubated the assays for 6 h at 30 °C in the presence of unlabeled ATP (100 μM). Phospho-specific immunoblots were quantified using Kodak Molecular Imaging software (New Haven, CT). Statistical significance of the *in vitro* kinase data was determined by one-tailed paired *t* test and defined as $p < 0.05$.

Mass Spectrometry (MS)—Gel bands containing *in vitro* phosphorylated i3 loop peptide or 5-HT$_{2A}$ receptor were washed/destained, reduced with dithiothreitol, alkylated with iodoacetamide, and digested overnight with an excess of modified trypsin using a standard in-gel digestion protocol. Peptides derived from the i3 loop were extracted from the polyacrylamide and concentrated for LC-tandem MS analysis. The liquid chromatography-mass spectrometry system was a ThermoFisher LTQ ion trap mass spectrometer (Thermo Electron Corp., Waltham, MA). Liquid chromatography was performed on an 8-cm × 75-μm inner diameter Phenomenex Jupiter C18 reversed-phase capillary chromatography column, packed in-house, coupled to the ThermoFisher LTQ mass spectrometer. Two-μl volumes of the extract were injected, and the peptides eluted from the column by an acetonitrile, 0.05 M acetic acid gradient at a flow rate of 0.2 μl/min were introduced into the source of the mass spectrometer on line. The digest was analyzed using the data-dependent multitask capability of the instrument acquiring full scan mass spectra to determine peptide molecular weights and product ion spectra to determine amino acid sequence in successive instrument scans.

Peptides derived from the 5-HT$_{2A}$ receptor were loaded onto a TiO_2 column (GL Sciences, Inc., Torrance, CA) for enrichment of phosphorylated peptides. Phosphopeptides were eluted with 3% ammonium hydroxide, then concentrated in a vacuum centrifuge to 2–3 μl, and adjusted to a final volume of 5 μl with 1% formic acid, 2% acetonitrile in water for liquid chromatography-mass spectrometry analysis. Liquid chromatography was performed on a MDLC nano-high pressure liquid chromatography system (GE Healthcare) coupled to the ThermoFisher LTQ mass spectrometer. The resulting peptides were loaded onto a 300-μm inner diameter × 5-mm C18 PepMap nano-reverse phase trapping column (Dionex, Sunnyvale, CA) to pre-concentrate and wash away excess salts. The loading flow rate was set to 25 μl/min, with 0.1% formic acid, pH 2.9, as the loading solvent. Reverse phase separation was performed on a 75-μm inner diameter × 15-cm C18, PepMap nano-separation column (Dionex, Sunnyvale, CA). Peptide separation was accomplished using buffer A (100% water and 0.1% formic acid) and buffer B (20% water, 80% acetonitrile, and 0.1% formic acid). Proteolytic peptide mixtures eluted from the col-

umn with the gradient of acetonitrile of 2% per min were introduced into the mass analyzer equipped with a nanospray ion source (2.2 kV).

The i3 loop peptide data were analyzed by a combination of two approaches to discover the phosphorylated peptides as follows. 1) All collision-induced dissociation (CID) spectra were used by the search program Sequest (Thermo Electron Corp., Waltham, MA) to search the 5-HT$_{2A}$ i3 loop amino acid sequence considering variable modification of Ser, Thr, and Tyr residues by 80 Da. 2) Neutral loss chromatograms were plotted to facilitate the recognition of CID spectra that contained the characteristic loss of phosphoric acid (H_3PO_4, −98 Da) from phospho-Ser- and phospho-Thr-containing peptides.

For the 5-HT$_{2A}$ receptor the Mascot search engine (Matrix Science, Boston, MA) was used to search the NCBI *Rattus* protein data base considering Ser, Thr, or Tyr phosphorylation. The first survey MS scan was performed in the positive ion mode. The second LTQ measurement was tandem MS of the four most intense peptide ions and MS-MS-MS (MS^3) of all ions showing the neutral loss of H_3PO_4 (−98 Da) from the precursor ion. All spectra were manually validated, and the following acceptance criteria were applied: all phospho-Ser and phospho-Thr peptides were required to show a pronounced neutral loss-dependent MS^3 scan and extensive coverage of b- and/or y-type series ions.

$^{32}P_i$ Metabolic Labeling—The cellular ATP pool was labeled with ^{32}P by incubating fibroblasts in phosphate-free DMEM for 1 h, followed by a 4-h incubation with phosphate-free DMEM containing 0.2 mCi/ml $^{32}P_i$. RSK2 was activated during the last hour of labeling by addition of 0.1 ng/ml EGF. 5-HT$_{2A}$ receptors were immunopurified from cell lysates using M2 FLAG affinity resin as described previously (28). Equal amounts of receptor were separated on a 10% SDS-polyacrylamide gel, dried, and imaged (BioMax MR, Kodak).

FLIPR Analysis of Intracellular Calcium Release—Intracellular calcium release was measured using a fluorometric imaging plate reader (FLIPRTetra) and calcium assay kit (Molecular Devices, Sunnyvale, CA). Briefly, 30,000 cells were plated into black wall, clear bottom 96-well tissue culture plates (Greiner Bio-One, Monroe, NC) in dialyzed culture medium (DMEM, 5% fetal bovine serum dialyzed to <0.05 nM 5-HT, 1 mM sodium pyruvate, 100 units/ml penicillin, and 100 μg/ml streptomycin). The cell culture medium was replaced with calcium assay buffer (20 mM HEPES, 1× HBSS, 2.5 mM probenecid, and calcium assay reagent, pH 7.4), incubated for 1 h at 37 °C, and equilibrated to room temperature before the assay. For EGF desensitization experiments, cells were incubated in serum-free medium (DMEM, 0.1% BSA, 100 units/ml penicillin, and 100 μg/ml streptomycin) >24 h before addition of calcium assay buffer. EGF (100 ng/ml) was diluted in assay buffer and added during the dye incubation step. The FLIPRTetra was programmed to add agonist ~10 s after establishing base-line relative fluorescence unit (RFU) values (excitation 470–495, emission 515–575 nm). RFU values were collected every second for 5 min, and the average base-line values were subtracted from maximum RFU values. Base-line subtracted values were normalized to cell number, expressed relative to the maximal wild-type 5-HT response, and analyzed by nonlinear regression (GraphPad). The *F* test was used to determine statistical significance of the fit parameters (potency, EC_{50} values, and efficacy, E_{max}), $p < 0.05$.

To normalize receptor expression, we treated cells with EEDQ (1–100 μM) for 30 min at 37 °C prior to incubation with FLIPR assay buffer. Cells were also treated in parallel with EEDQ (1–100 μM) prior to preparation of membranes for quantification of receptor expression (20). Concentrations of EEDQ that produced equal levels of receptor expression between cell lines were compared for their agonist responses in the FLIPR assay.

Analysis of Inositol Phosphates—The ^3H Biotrak assay system (Amersham Biosciences) was used exactly as described by the manufacturer to detect inositol 1,4,5-trisphosphate (IP_3). Initially we measured inositol phosphate (IP) accumulation using anion-exchange chromatography as detailed previously (20, 34). Subsequent measurements of IP were made using the scintillation proximity assay method (35). Briefly, 30,000 cells were plated into 96-well tissue culture plates in dialyzed culture medium. The cells were briefly inositol-starved (1.5 h) and incubated for 18 h at 37 °C with labeling medium (inositol-free basal medium Eagle, 5% dialyzed fetal bovine serum, and 0.01 μCi/μl [^3H]myoinositol). The labeling medium was removed, and agonists diluted in assay buffer (1× HBSS, 24 mM $NaHCO_3$, 11 mM glucose, and 35 mM LiCl, pH 7.4) were added to the cells for 1 h at 37 °C. The assay was terminated by addition of 50 mM formic acid, and the supernatant was incubated with 0.2 mg of yttrium silicate beads (YSi, Amersham Biosciences). Radioactivity was measured by scintillation counting (Wallac Microbeta TriLux, PerkinElmer Life Sciences). Base-line subtracted values were normalized to cell number, expressed relative to the maximal wild-type 5-HT response, and analyzed by nonlinear regression (GraphPad). The *F* test was used to determine statistical significance of the fit parameters (EC_{50} and E_{max}), $p < 0.05$. Statistical significance of IP_3 time course data were determined by one-tailed paired *t* test and defined as $p < 0.05$.

RESULTS

RSK2 N-terminal Kinase Activity Is Required for 5-HT$_{2A}$ Receptor Regulation—We have previously shown that the Ser/Thr kinase RSK2 interacts with the 5-HT$_{2A}$ receptor i3 loop in a conserved region containing the RSK2-like phosphorylation motif ^{275}RAKL(A/S)S^{280} (conserved across rat, human, and mouse; see Fig. 2*A*) (21). This sequence closely resembles the optimal RSK2 motif R*X*R*XX*S (23). Our previous work has also shown that RSK2 negatively regulates 5-HT$_{2A}$ signaling in fibroblasts, and as presented here, it occurs not only during the initial phase of signaling (0–90 s) but also during extended periods of signaling (0–60 min) (Fig. 1, *A* and *B*). Control studies have indicated that this negative regulation occurs independently of alterations distal to receptor activation such as changes in $G\alpha_q$ activity and receptor trafficking. Therefore, we focused our initial efforts on determining whether RSK2 regulates 5-HT$_{2A}$ signaling proximal to receptor activation, perhaps by directly phosphorylating the 5-HT$_{2A}$ receptor. A previous bioinformatic analysis suggested that Ser/Thr kinases could potentially phosphorylate more than 30 intracellular Ser/Thr residues on the 5-HT$_{2A}$ receptor (34). The alternative hypoth-

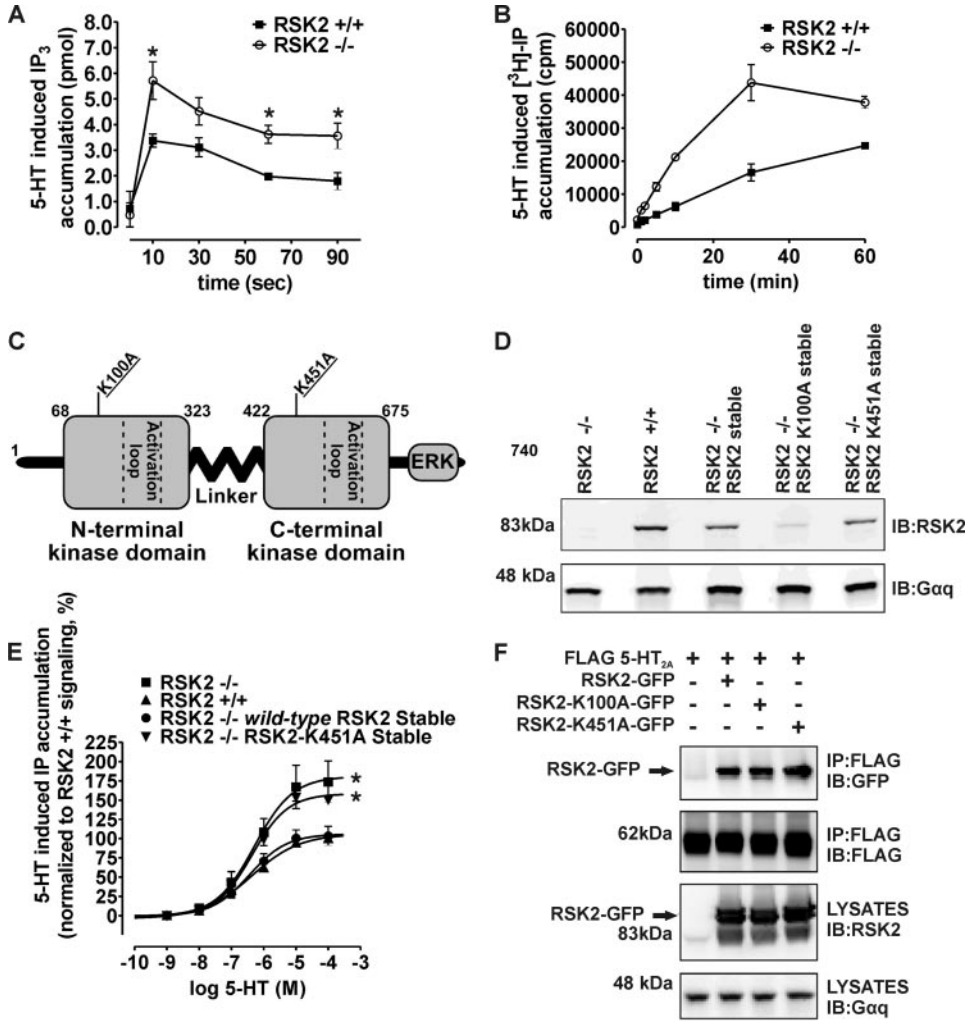

FIGURE 1. **RSK2 kinase activity is essential for negatively regulating 5-HT$_{2A}$ receptor signaling.** For time course experiments, IP_3 (*A*) and IP (*B*) were measured in RSK2$^{+/+}$ and RSK2$^{-/-}$ fibroblasts stably expressing 5-HT$_{2A}$ receptors following 10 μM 5-HT treatment. Wild-type or kinase-dead (K100A or K451A) RSK2 constructs (*C* and *D*) were expressed in RSK2$^{-/-}$ fibroblasts for rescue experiments (*E*) or HEK 293T cells for co-immunoprecipitations (*F*). *A*, rapid (0–90 s) 5-HT-mediated IP_3 production was significantly potentiated in RSK2$^{-/-}$ fibroblasts (○) when compared with RSK2$^{+/+}$ fibroblasts (■). Shown here are results from three independent experiments; *, $p < 0.05$. *B*, prolonged (0–60 min) 5-HT treatment led to increased production of IP in RSK2$^{-/-}$ fibroblasts (○) when compared with RSK2$^{+/+}$ fibroblasts (■). Shown here are results from three independent experiments. *C*, diagram illustrating overall structure of murine RSK2 and arrangement of RSK2 kinase domains. The Lys to Arg mutation within the ATP binding pocket of each kinase domain inactivates RSK2. *D*, Western blot analysis of cell lysates using an antibody specific to RSK2 shows similar RSK2 expression levels in RSK2$^{-/-}$ wild-type and RSK2$^{-/-}$ K451A fibroblast cell lines. *E*, stimulation of fibroblast cell lines with 5-HT (1 nM to 100 μM) shows concentration-dependent accumulation of [^{3}H]phosphoinositides from [^{3}H]phosphatidylinositol 4,5-bisphosphate hydrolysis. Disruption of kinase activity in RSK2-K451A fibroblasts (▼) failed to significantly attenuate maximal 5-HT$_{2A}$ signaling to levels seen with fibroblasts expressing endogenous RSK2 (▲) or RSK2$^{-/-}$ fibroblasts ectopically expressing wild-type RSK2 (●). The RSK2-K451A fibroblasts (▼) signaled similarly to RSK2$^{-/-}$ fibroblasts (■), thus suggesting that RSK2 kinase activity is essential for 5-HT$_{2A}$ regulation. These data were normalized to dpm/mg total protein where RSK2$^{+/+}$ fibroblast maximal signaling is set to 100% and represent four independent experiments; *, $p < 0.05$ when compared with RSK2$^{+/+}$ fibroblasts. *F*, FLAG-5-HT$_{2A}$ receptors were co-transfected with wild-type or kinase-dead RSK2 constructs fused to GFP in HEK 293T cells. GFP was used in this case to separate endogenous RSK2 from exogenous RSK2 (*arrow, lower panel*). Both wild-type and kinase-dead RSK2 proteins co-immunopurified with FLAG 5-HT$_{2A}$ as detected by an antibody against GFP (*arrow, top panel*). Shown are representative immunoblots from a single experiment that was replicated three times with equivalent results. *IP*, immunoprecipitation; *IB*, immunoblot.

esis is that RSK2 binds to 5-HT$_{2A}$ receptors and inhibits signaling via abrogating the interaction between 5-HT$_{2A}$ receptors and Gα subunits.

To determine whether RSK2 acts via direct phosphorylation, rather than a receptor-scaffolding action, we ectopically expressed wild-type RSK2, N-terminal kinase-dead RSK2 (K100A), or C-terminal kinase-dead RSK2 (K451A) constructs in RSK2$^{-/-}$ fibroblasts (Fig. 1*C*). Previous studies demonstrate that mutations at these sites in RSK2 eliminate the function of each kinase domain and ultimately lead to decreased substrate phosphorylation (36–39), thus allowing us to isolate and investigate the importance of RSK2 kinase activity. Indeed, if RSK2 kinase activity is required for regulating receptor signaling, we expected that re-introduction of wild-type RSK2, but not the kinase-dead RSK2 constructs, into RSK2$^{-/-}$ fibroblasts would attenuate receptor signaling in a manner similar to RSK2$^{+/+}$ fibroblasts.

Western blot analysis demonstrated that RSK2$^{-/-}$ fibroblasts stably transduced with the wild-type RSK2 and RSK2-K451A constructs, but not the RSK2-K100A mutant, expressed similar amounts of RSK2 when compared with RSK2$^{+/+}$ fibroblasts (Fig. 1*D*). Despite numerous attempts, we were unable to express the RSK2-K100A mutant at levels equivalent to wild type and, instead, pursued further studies with the RSK2-K451A mutant. We measured agonist-mediated 5-HT$_{2A}$ receptor activity via [^{3}H]phosphatidylinositol 4,5-bisphosphate hydrolysis and found that RSK2$^{-/-}$ fibroblasts expressing wild-type RSK2, but not kinase-dead RSK2 (K451A), attenuated agonist-mediated 5-HT$_{2A}$ signaling to a level indistinguishable from that observed in RSK2$^{+/+}$ fibroblasts (Fig. 1*E* and Table 1). These results implied that RSK2 kinase activity was necessary for regulating 5-HT$_{2A}$ receptor signaling.

We next performed control studies to determine whether the kinase-dead mutants maintained interactions with 5-HT$_{2A}$ receptors, because it is conceivable that RSK2 modulates 5-HT$_{2A}$ signaling via direct interaction with the 5-HT$_{2A}$ receptor and not via receptor phosphorylation. For these studies we utilized GFP-tagged wild-type RSK2 (RSK2-GFP) and kinase-dead RSK2 (RSK2-K100A-GFP and RSK2-K451A-GFP) co-expressed with epitope-tagged 5-HT$_{2A}$ receptors (FLAG 5-HT$_{2A}$) in HEK

293T cells. As is shown in Fig. 1*F*, both GFP-tagged kinase-dead RSK2 mutants interacted with 5-HT$_{2A}$ receptors to the same extent as GFP-tagged wild-type RSK2 (*arrow, top panel*). Taken together, these results demonstrate that a direct physical interaction between 5-HT$_{2A}$ receptors and RSK2 is insufficient to modulate signaling, because kinase-dead mutants interact with the 5-HT$_{2A}$ receptor but do not rescue the RSK2$^{-/-}$ signaling phenotype. Given that RSK2 interacts with 5-HT$_{2A}$ receptors *in vitro* and the 5-HT$_{2A}$ i3 loop contains an RSK2-like consensus site, the most likely explanation for our results is that RSK2 modulates 5-HT$_{2A}$ signaling via receptor phosphorylation. We then investigated the potential for RSK2-mediated 5-HT$_{2A}$ receptor phosphorylation.

TABLE 1
Effects of ectopically expressed wild-type and kinase-dead RSK2 on endogenous 5-HT$_{2A}$ receptor signaling in mouse embryonic fibroblasts

Cell line	Agonist potency[a] EC_{50} (pEC_{50} ± S.E.[b])	Relative agonist efficacy[a] % E_{max} ± S.E.
RSK2$^{+/+}$ fibroblasts	411 nM (6.39 ± 0.12)	106 ± 5
RSK2$^{-/-}$ fibroblasts	515 nM (6.29 ± 0.28)	181 ± 20[c]
RSK2$^{-/-}$ wild-type RSK2-stable	368 nM (6.44 ± 0.21)	107 ± 9
RSK2$^{-/-}$ RSK2-K451A-stable	436 nM (6.36 ± 0.13)	158 ± 8[c]

[a] Agonist potencies (EC_{50}) and efficacies (E_{max}) were determined for 5-HT-mediated IP accumulation. The results represent the average of four independent experiments.
[b] pEC_{50} values are represented as −log of EC_{50} in molar.
[c] Values are statistically different from RSK2$^{+/+}$ fibroblasts, $p < 0.05$.

RSK2 Phosphorylates the 5-HT$_{2A}$ Receptor in Vitro—We initially carried out kinase experiments *in vitro* to determine whether purified RSK2 can directly phosphorylate purified 5-HT$_{2A}$ receptors. We created a tandem affinity-tagged 5-HT$_{2A}$ receptor (Fig. 2*A*) and found that the addition of N-terminal affinity tags did not perturb overall receptor conformation because the affinity-tagged receptor bound [^{3}H]ketanserin with a K_d equal to 2.65 ± 0.39 nM ($n = 4$), consistent with reported affinities for the 5-HT$_{2A}$ receptor. As shown in Fig. 2*B*, RSK2 autophosphorylation demonstrated that our *in vitro* assay conditions retained RSK2 kinase activity (*arrow* ~88 kDa), as reported by others (40). Incubation of purified 5-HT$_{2A}$ receptors with activated RSK2 and [γ-^{32}P]ATP resulted in robust [^{32}P]phosphate incorporation into the 5-HT$_{2A}$ receptor (Fig. 2*B*, *arrow* at ~62 kDa) relative to control assays lacking RSK2 (Fig. 2, *B* and *C*). Importantly, the selective RSK inhibitor SL0101, used at a concentration that inhibits >75% of RSK2 N-terminal kinase activity (41), blocked phosphorylation (Fig. 2*C*). Thus, incubation with 10 μM SL0101 attenuated 5-HT$_{2A}$ phosphorylation to levels approaching the control assay lacking RSK2 (175 ± 41% *versus* 474 ± 148% increase in [^{32}P]phosphate incorporation in the presence and absence of SL0101, respectively; $p < 0.05$, $n = 4$). We further confirmed that inhibition of the N-terminal kinase domain of RSK2 attenuated 5-HT$_{2A}$ receptor phosphorylation by obtaining identical results with 100 nM of the selective RSK inhibitor BI-D1870 (data not shown), a concentration that inhibits 98% of RSK2 N-terminal kinase activity (42). Because the N-terminal kinase domain of RSK2 is responsible for substrate phosphorylation, a significant decrease in 5-HT$_{2A}$ phosphorylation upon application of these specific RSK inhibitors supports our conclusion that activated and purified RSK2 phosphorylates the 5-HT$_{2A}$ receptor *in vitro*.

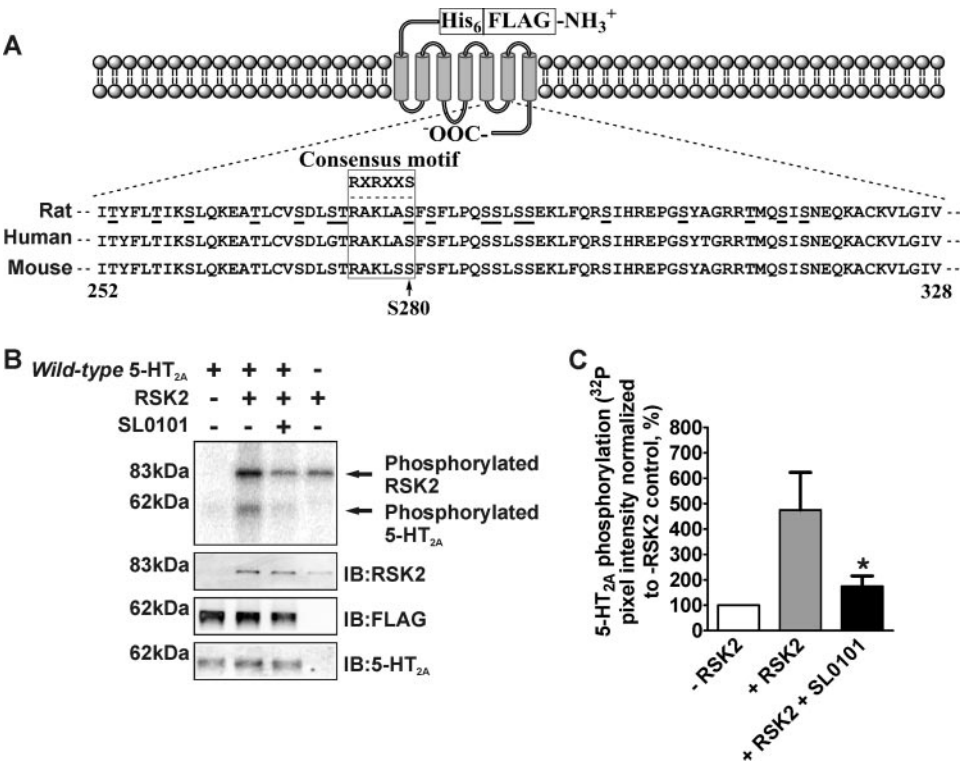

FIGURE 2. **RSK2 phosphorylates the 5-HT$_{2A}$ receptor *in vitro*.** For these experiments purified FLAG-His$_6$ 5-HT$_{2A}$ receptors (*A*) were phosphorylated *in vitro* using purified, activated RSK2 (*B* and *C*). *A*, diagram illustrating design of the tandem affinity-tagged 5-HT$_{2A}$ receptor and alignment of rat, human, and mouse i3 loop amino acid sequences. Potential Ser or Thr phosphorylation sites are *underlined*, and the RSK2-like consensus phosphorylation motif is *boxed* with the optimal sequence shown *above*. *B*, FLAG-His$_6$ 5-HT$_{2A}$ receptor was phosphorylated *in vitro* as described under "Experimental Procedures." The *top panel* is a representative phosphorimage showing RSK2-mediated incorporation of [^{32}P]phosphate into the 5-HT$_{2A}$ receptor (*arrow* at ~62 kDa). The presence of the specific RSK inhibitor 10 μM SL0101 blocked [^{32}P]phosphate incorporation into the 5-HT$_{2A}$ receptor. Western blot analysis of the samples loaded for phosphorimager detection (*lower panels*) confirmed the components of each *in vitro* kinase assay. *IB*, immunoblot. *C*, quantification of 5-HT$_{2A}$ receptor phosphorylation shown in *B*. The sum pixel intensity values from phosphorimager bands were normalized to control assays lacking RSK2 (set to 100%). These data show that SL0101 significantly decreased RSK2-mediated [^{32}P]phosphate incorporation into the 5-HT$_{2A}$ receptor. Shown here are results from four independent experiments; *, $p < 0.05$.

RSK2 Phosphorylates the 5-HT$_{2A}$ Receptor I3 Loop—We previously showed that the 5-HT$_{2A}$ i3 loop interacts with RSK2, contains a conserved RSK2-like consensus phosphorylation motif (^{275}RAKLAS^{280}, *boxed* in Fig. 2*A*), and is implicated in G protein coupling (2, 21). Thus

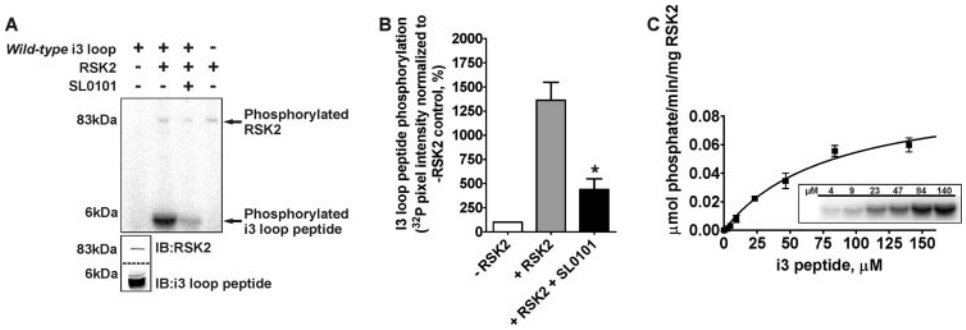

FIGURE 3. **RSK2 phosphorylates the 5-HT$_{2A}$ receptor third intracellular (i3) loop *in vitro*.** For these experiments purified i3 loop peptides were phosphorylated *in vitro* with purified, activated RSK2. *A,* i3 loop peptide was phosphorylated *in vitro* as described under "Experimental Procedures." The *top panel* is a representative phosphorimage showing RSK2-mediated incorporation of [^{32}P]phosphate into the i3 loop peptide (*arrow* at ~6 kDa). The *arrow* at ~88 kDa denotes RSK2 autophosphorylation. The *lower panels* show Western blot validation of RSK2 and i3 loop peptide mobilities. *IB*, immunoblot. *B,* quantification of 5-HT$_{2A}$ receptor i3 loop phosphorylation shown in *A*. The sum pixel intensity values from phosphorimager bands were normalized to control assays lacking RSK2 (set to 100%). These data show that SL0101 significantly decreased RSK2-mediated [^{32}P]phosphate incorporation into the i3 loop peptide. Shown here are results from three independent experiments; *, $p < 0.05$. *C,* kinetic analysis of i3 loop phosphorylation. *In vitro* kinase assays using increasing concentrations of i3 loop peptide (2.3 to 140 μM, *inset*) were performed under initial velocity conditions. Radioactive bands were excised and quantified by liquid scintillation counting. Background subtracted values were plotted against i3 loop peptide concentrations and fit to a one-site hyperbolic equation to determine V_{max} and K_m.

we next determined if RSK2 can phosphorylate the i3 loop using *in vitro* kinase assays incorporating [γ-^{32}P]ATP, purified i3 loop peptide (*amino acids 252–328,* Fig. 2*A*), and purified, activated RSK2. Consistent with our results using the full-length 5-HT$_{2A}$ receptor, activated RSK2 robustly incorporated [^{32}P]phosphate into the purified i3 loop peptide relative to control assays lacking RSK2 (Fig. 3*A*). PhosphorImager quantification in Fig. 3*B* shows that 10 μM SL0101 attenuated phosphorylation (440 ± 109% *versus* 1360 ± 186% increase in [^{32}P]phosphate incorporation in the presence and absence of SL0101, respectively; $p < 0.05$, $n = 3$). These data show that the i3 loop is an RSK2 substrate *in vitro*. We further determined the kinetics of i3 loop phosphorylation by measuring [^{32}P]phosphate incorporation into i3 loop peptide (2.3–140 μM). These experiments were performed under initial velocity conditions in which the i3 loop peptide substrate was not depleted, and the detection system was not saturated (data not shown). As shown in Fig. 3*C*, RSK2 phosphorylated the i3 loop peptide with saturable kinetics resulting in a maximal reaction rate (V_{max}) equal to 0.099 ± 0.012 μmol P·min^{-1}·mg^{-1} RSK2 and an estimate of affinity (K_m) equal to 81.8 ± 19.6 μM. These results demonstrate that RSK2 robustly phosphorylates the 5-HT$_{2A}$ receptor i3 loop *in vitro* with an affinity similar to that previously reported for the RSK2 peptide substrate KKRNKTLSVA (23).

RSK2 Specifically Phosphorylates the Conserved Residue Ser-314 within the 5-HT$_{2A}$ Receptor I3 Loop—To validate our *in vitro* data and to otherwise rule out stochastic, nonspecific phosphorylation events that can occur with *in vitro* kinase assays, we searched for phospho-acceptor sites within the *in vitro* phosphorylated 5-HT$_{2A}$ receptor i3 loop. The 5-HT$_{2A}$ receptor i3 loop contains 18 potential phosphorylation sites for Ser/Thr kinases (*underlined* in Fig. 2*A*), and conceivably, any of these sites could be phosphorylated. Therefore, we chose the unbiased approach of tandem MS to efficiently explore i3 loop phosphorylation space. The sequence coverage for trypsin digestion of the i3 loop peptide was 81% (*underlined* in Fig. 4*A*), and we were unable to account for only one Ser and one Thr located in the i3 loop N terminus. Analysis of the CID spectra obtained from the kinase-treated i3 loop peptide found a total of four peptides that corresponded to putative phosphorylation sites. The first site, corresponding to Ser-314 (100% conserved among rat, human, and mouse 5-HT$_{2A}$ receptors, see Fig. 2*A*), was identified in two consecutive experiments from the peptides ^{311}TMoQpSISNEQK^{320} and ^{310}RTMoQpSISNEQK^{320} (where Mo is an oxidized Met and pS represents phospho-Ser). The CID spectrum of the ^{311}TMoQpSISNEQK^{320} peptide is shown in Fig. 4*A*. This spectrum has the expected abundant ion from the loss of H_3PO_4 (−98Da) and, particularly in the case of the ^{311}TMoQpSISNEQK^{320} peptide, sufficient information to establish the site of phosphorylation. Mass chromatograms were plotted for these ions that clearly showed the detection of both forms of the phosphopeptide in the kinase-treated sample and the absence of the peptides in the control sample without kinase (data not shown). A second minor phosphorylation site (Ser-280) was also observed that corresponds to the phosphopeptide ^{278}LApSFSFLPQSSLSSEK^{293} that contains the phosphorylated Ser in the RSK2-like consensus phosphorylation motif (data not shown). Again, a prominent ion from the loss of H_3PO_4 was observed. Furthermore, significant sequence-specific ions were observed to verify the correct peptide. The exact site of phosphorylation is less clear and was determined with an MS^3 experiment in which the fragment ion from the loss of H_3PO_4 was refragmented, and a pair of low abundance y-ions was observed that corresponded to the expected dehydro-Ala. However, the significance of this site is questionable because this phosphopeptide was only detected in one of the experiments and was present in both the kinase-treated sample and control sample without kinase indicating that its formation was independent of kinase treatment. Two exceedingly low abundance phosphopeptides were also identified, ^{264}EATLCVSDLSTR^{275} and ^{298}SIHREPGSYAGR^{309} (data not shown). These spectra contained only a limited amount of sequence information because of the abundant ion from the loss of H_3PO_4. These peptides were not seen in all of our experiments, and this lack of reproducibility would lessen the potential significance of these sites. We report these sites here for completeness.

We verified our MS phosphorylation assignment using two independent methods. First, we used site-directed mutagenesis to generate Ser to Ala mutants at both MS assigned sites (S280A and S314A), thus rendering each site phosphorylation-deficient. As shown in Fig. 4*B* and quantified in Fig. 4*C*, activated RSK2 incorporated [^{32}P]phosphate into the wild-type and the S280A mutant peptides to a similar extent relative to control assays lacking RSK2 (978 ± 213 and 1010 ± 152% increase in

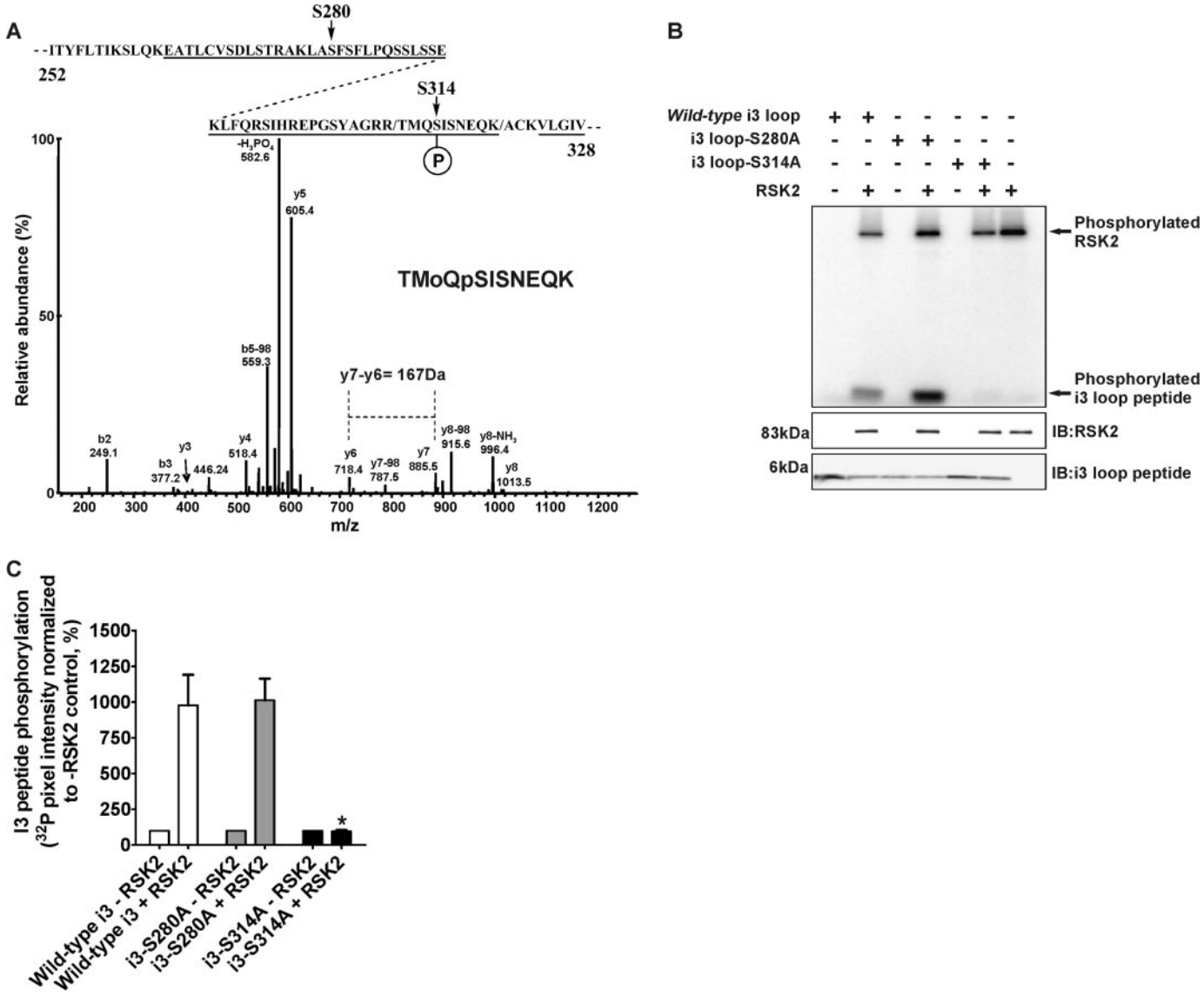

FIGURE 4. **RSK2 specifically phosphorylates Ser-314 within the 5-HT$_{2A}$ receptor i3 loop.** For these experiments purified 5-HT$_{2A}$ i3 loop peptides were phosphorylated *in vitro* with purified, activated RSK2, and phosphate incorporation was subsequently analyzed by MS (*A*) and [^{32}P]phosphate incorporation (*B* and *C*). *A,* tandem MS analysis of *in vitro* phosphorylated wild-type i3 peptide identified Ser-280 and Ser-314 as putative phosphorylation sites (*arrows, top diagram*). The CID spectrum of the reproducible and robust phosphopeptide ^{311}TMoQpSISNEQK^{320} is shown, where Mo represents oxidized Met and pS represents phospho-Ser-314. Although the CID spectrum contains an abundant ion because of the loss of H_3PO_4 (−98Da) that is characteristic of Ser phosphorylation, sufficient information to place the site of phosphorylation is also observed. Specifically the mass difference of 167 Da between y-series ions y_6 and y_7 corresponds to phospho-Ser-314. *B,* site-directed mutagenesis of Ser-280 (S280A) and Ser-314 (S314A) indicates that RSK2 predominantly phosphorylates Ser-314. Western blot analysis of the samples loaded for phosphorimager detection (*lower panels*) confirmed the components of each *in vitro* kinase assay. *IB,* immunoblot. *C,* quantification of i3 loop peptide phosphorylation shown in *B*. The sum pixel intensity values from phosphorimager bands were normalized to control assays lacking RSK2 (set to 100%). The S314A mutation completely abolished [^{32}P]phosphate incorporation into the i3 loop when compared with the wild-type peptide. Shown here are results from three independent experiments; *, $p < 0.05$.

[^{32}P]phosphate incorporation for wild-type and S280A peptides, respectively; $p > 0.05$, $n = 3$). However, the S314A mutation completely abolished RSK2-mediated phosphorylation when compared with [^{32}P]phosphate incorporation for the wild-type peptide (95.0 ± 10.9% *versus* 978 ± 213% increase in [^{32}P]phosphate incorporation for S314A and wild-type peptides, respectively; $p < 0.05$, $n = 3$). Taken together, our results using phosphorylation-deficient i3 peptides support the robust MS assignment at Ser-314 and show that the minor Ser-280 site does not significantly contribute to phosphorylation *in vitro*. We also tested the phosphorylation sites found in the low abundance phosphopeptide ^{298}SIHREPGSYAGR^{309} (S298A and S305A) and found that neither mutation inhibited RSK2 phosphorylation (data not shown).

We further validated our MS assignment by generating a phospho-specific antibody against phospho-Ser-314 (Ser(P)-314 Ab) to probe *in vitro* kinase assays. Initial dot blot experiments demonstrated that the Ser(P)-314 Ab selectively detects <10 ng of the phosphorylated antigenic peptide (Fig. 5*A, bottom panel*). As shown in Fig. 5*A* and quantified in Fig. 5*B*, we detected a large increase in Ser(P)-314 Ab immunolabeling when the wild-type i3 loop peptide was incubated with activated RSK2. In support of the selectivity of the Ser(P)-314 Ab, and consistent with our Ala mutagenesis data, the phospho-

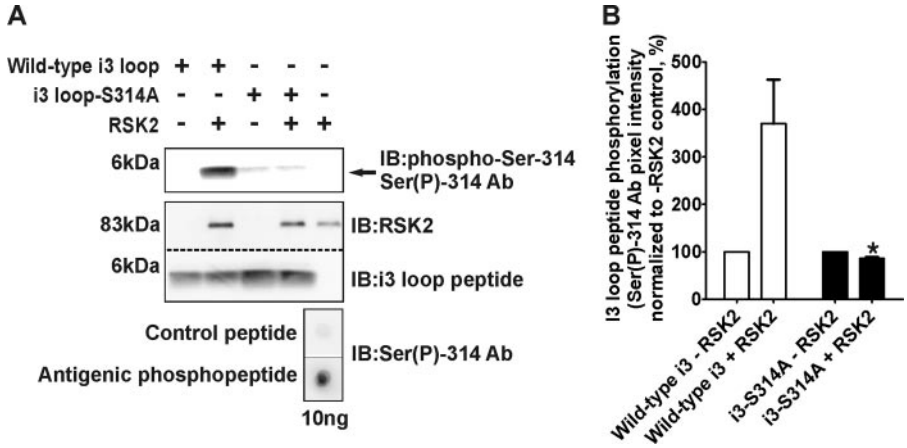

FIGURE 5. **The phospho-Ser-314-specific antibody validates Ser-314 phosphorylation within the 5-HT$_{2A}$ receptor i3 loop.** For these experiments purified wild-type and phosphorylation-deficient (i3-S314A) i3 loop peptides were phosphorylated *in vitro* with purified, activated RSK2 and subsequently immunoblotted (*IB*) with the phospho-Ser-314-specific antibody (Ser(P)-314 Ab, *bottom panel* shows specificity). *A,* Ser(P)-314 Ab immunolabeling shows that activated RSK2 phosphorylates the wild-type i3 loop peptide (*top panel*, *arrow* at ~6 kDa). Inability of the Ser(P)-314 Ab to detect *in vitro* phosphorylated i3-S314A peptide indicates the lack of phosphorylation at this site and specificity of the Ab. Western blot analysis of the samples loaded for Ser(P)-314 Ab detection (*lower panels*) confirmed the components of each *in vitro* kinase assay. *B,* quantification of Ser(P)-314 Ab immunolabeling shown in *A*. The sum pixel intensity values from i3 loop peptide bands (*top panel, A*) were normalized to control assays lacking RSK2 (set to 100%). The S314A mutation completely abolished immunolabeling of the Ser(P)-314 Ab when compared with the wild-type peptide. Shown here are results from three independent experiments; *, $p < 0.05$.

specific Ab failed to immunolabel the phosphorylation-deficient i3 loop peptide (i3-S314A) when compared with the wild-type i3 loop peptide (86.0 ± 2.7% *versus* 370 ± 93% increase in control pixel intensity for the S314A and wild-type i3 peptides, respectively; $p < 0.05$, $n = 3$). We also generated and validated a phospho-specific Ab of similar sensitivity against phospho-Ser-280, and consistent with our Ala mutagenesis data, we failed to detect significant phosphorylation at Ser-280 (data not shown). Taken together, our MS, site-directed mutagenesis, and phospho-specific immunoblotting results unambiguously show that RSK2 specifically phosphorylates Ser-314 within the 5-HT$_{2A}$ receptor i3 loop *in vitro*.

RSK2 Specifically Phosphorylates the Full-length 5-HT$_{2A}$ Receptor at Ser-314—The i3 loop peptide studies clearly demonstrate that activated RSK2 phosphorylates Ser-314 *in vitro*. However, because this result was achieved using only the i3 loop fragment of the 5-HT$_{2A}$ receptor, we needed to validate this with intact, full-length receptor. Accordingly, we developed an unbiased strategy to probe RSK2 phosphorylation space similar to our i3 loop peptide experiments. Here we interrogated *in vitro* receptor phosphorylation using tandem MS, the Ser(P)-314 Ab, and $^{32}P_i$ metabolic labeling. As shown in the tandem MS of a doubly charged phospho-Ser-containing peptide ^{311}TMQpSISNEQK^{320} with *m/z* of 623.5, we detected phosphorylation at Ser-314 in the intact receptor (Fig. 6*A*). Phosphorylation at Ser-314 was confirmed by the detection of dehydro-Ala in the sequence because of the loss of H_3PO_4 (−98 Da) by β-elimination. Specifically, for the b-type series, b_{4-9} fragments clearly show both the mass shifts of +80 Da and loss of H_3PO_4 (−98 Da), whereas b_2 and b_3 ions are unchanged upon comparison with the spectrum of unmodified peptide. The y-type series ions y_{2-6} show no modification, whereas for y_{7-8} fragment ions both the mass shifts of +80 Da and loss of H_3PO_4 (−98 Da) are observed. Moreover, we observed a mass difference of 167 Da between y-type series ions y_6 and y_7 and b-type series ions b_3 and b_4, corresponding to a phospho-Ser. Therefore, we can confidently assign phosphorylation to the conserved Ser-314 in the intact 5-HT$_{2A}$ receptor (Fig. 6*B*).

We subsequently validated the MS assignment using the following: 1) the Ser(P)-314 Ab to probe for phospho-Ser-314 under conditions that resulted in 5-HT$_{2A}$ receptor phosphorylation *in vitro*, and 2) $^{32}P_i$ metabolic labeling in intact fibroblasts stably expressing wild-type or phosphorylation-deficient (5-HT$_{2A}$-S314A) 5-HT$_{2A}$ receptors. As shown in Fig. 7*A* and quantified in Fig. 7*B*, we detected a large increase in Ser(P)-314 Ab immunolabeling following *in vitro* phosphorylation of the 5-HT$_{2A}$ receptor with activated RSK2. Additionally, we attenuated Ser(P)-314 Ab recognition, and by extension 5-HT$_{2A}$ phosphorylation, using the selective RSK inhibitor SL0101 (112 ± 5% *versus* 138 ± 8% increase in control pixel intensity in the presence and absence of SL0101, respectively; $p < 0.05$, $n = 5$). This result was internally consistent with our previous experiments using both the full-length receptor (Fig. 2) and i3 loop peptide (Fig. 3) in which the selective RSK inhibitor significantly attenuated [^{32}P]phosphate incorporation.

Metabolic labeling of proteins has been the "gold standard" method for elucidating phosphorylation of numerous GPCRs in intact cells including the β-adrenergic and μ- and δ-opioid receptors (43–47). Here we used this approach to probe 5-HT$_{2A}$ phosphorylation in whole cells by immunopurifying wild-type and 5-HT$_{2A}$-S314A receptors from $^{32}P_i$-labeled fibroblasts following EGF activation of RSK2 (48, 49). Both the wild-type 5-HT$_{2A}$ and 5-HT$_{2A}$-S314A polyclonal cell lines bound [^{3}H]ketanserin with K_d values consistent with reported affinities for the 5-HT$_{2A}$ receptor (wild-type 5-HT$_{2A}$ K_d = 3.08 ± 0.45 nM, $n = 3$; 5-HT$_{2A}$-S314A K_d = 3.18 ± 0.50 nM, $n = 4$) and expressed similar amounts of receptor (wild-type 5-HT$_{2A}$ B_{max} = 703 ± 190 fmol/mg protein, 5-HT$_{2A}$-S314A B_{max} = 818 ± 106 fmol/mg protein). As shown in Fig. 7*C*, EGF time-dependently activated endogenous RSK2 in these fibroblasts with maximal activation occurring at 10 min. Autoradiographic analysis of receptors immunopurified from EGF-activated, $^{32}P_i$-labeled fibroblasts detected receptor phosphorylation in the wild-type 5-HT$_{2A}$ fibroblasts but failed to detect phosphorylation in 5-HT$_{2A}$-S314A fibroblasts and control fibroblasts lacking the tagged receptor (*arrow* at ~62 kDa, Fig. 7*D*). These results, taken together with the previous *in vitro* data, show that activated RSK2 specifically phosphorylates Ser-314 within the 5-HT$_{2A}$ receptor i3 loop *in vitro* and in intact cells.

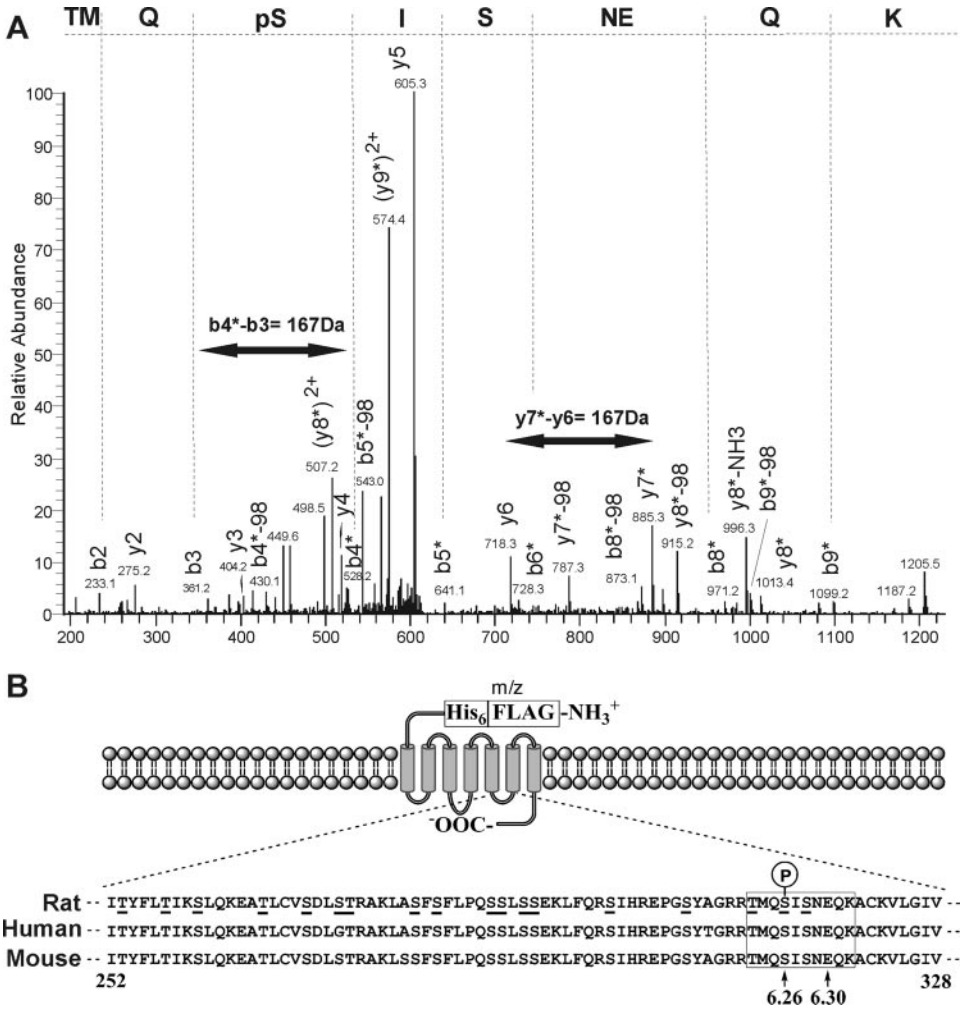

FIGURE 6. **RSK2 phosphorylates the full-length 5-HT$_{2A}$ receptor at Ser-314 *in vitro*.** For these experiments purified FLAG-His$_6$ 5-HT$_{2A}$ receptors were phosphorylated *in vitro* using purified, activated RSK2 and analyzed by tandem MS (*A*) to identify phosphorylation site(s) in the full-length receptor (*B*). *A,* phosphopeptides derived from *in vitro* phosphorylated receptors were concentrated and analyzed as described under "Experimental Procedures." Shown here is the tandem MS chromatogram of the phosphopeptide ^{311}TMQpSISNEQK^{320}, where pS represents phospho-Ser-314. Phosphorylation at Ser-314 was confirmed by the detection of dehydro-Ala in the sequence because of the loss of the H_3PO_4 (−98 Da) by β-elimination in both b- and y-series fragment ions. We also observed a mass difference of 167 Da between y-type series ions y_6 and y_7, and b-type series ions b_3 and b_4 (*double-headed arrows*, corresponds to phospho-Ser-314). *B,* diagram illustrating location of Ser-314 (6.26, *arrow*) within the i3 loop in relation to Glu-318(6.30, *arrow*), which is necessary for maintaining the 5-HT$_{2A}$ receptor in an inactive conformation.

RSK2 Requires Ser-314 within the 5-HT$_{2A}$ Receptor i3 Loop for Regulating Agonist Signaling—Our data unequivocally show that RSK2 phosphorylates the conserved Ser-314 within the i3 loop. To determine whether RSK2 requires Ser-314 phosphorylation to regulate 5-HT$_{2A}$ receptor signaling, we compared the stable fibroblast cell lines previously used for metabolic labeling experiments (wild-type 5-HT$_{2A}$ and phosphorylation-deficient 5-HT$_{2A}$-S314A) at multiple agonist-induced 5-HT$_{2A}$ signaling pathways (*i.e.* intracellular Ca^{2+} release and IP accumulation). Because RSK2 phosphorylated Ser-314 *in vitro* and in intact cells, we predicted that phosphorylation-deficient 5-HT$_{2A}$-S314A receptor signaling would be insensitive to endogenous RSK2 modulation and should exhibit increased signaling similar to our observations in RSK2$^{-/-}$ fibroblasts (Fig. 1*E*).

Consistent with our prediction, all three 5-HT$_{2A}$ receptor agonists (*i.e.* 5-HT, DOI, and α-Me5-HT) exhibited increased efficacy and potency in the phosphorylation-deficient 5-HT$_{2A}$-S314A fibroblasts when compared with the wild-type 5-HT$_{2A}$ fibroblasts (Table 2). Specifically, all three 5-HT$_{2A}$ receptor agonists mobilized significantly more intracellular Ca^{2+} in the 5-HT$_{2A}$-S314A fibroblasts when compared with the wild-type 5-HT$_{2A}$ fibroblasts (Fig. 8*A* and Table 2). Potencies for all 5-HT$_{2A}$ agonists were significantly increased (2–4-fold) in the 5-HT$_{2A}$-S314A fibroblasts. Similarly, all three 5-HT$_{2A}$ receptor agonists accumulated significantly more IP in the 5-HT$_{2A}$-S314A fibroblasts when compared with the wild-type 5-HT$_{2A}$ fibroblasts (Fig. 8*B* and Table 2). Agonist potencies for IP accumulation also significantly increased in 5-HT$_{2A}$-S314A fibroblasts (2-fold). Because we are using polyclonal stable lines, it is possible that differences in receptor expression between the wild-type 5-HT$_{2A}$ and 5-HT$_{2A}$-S314A polyclonal stable lines could account for increased 5-HT$_{2A}$-S314A receptor signaling. Thus we developed a method that simultaneously normalized receptor expression and measured agonist-induced intracellular Ca^{2+} release. We found that at concentrations of EEDQ that produced equivalent levels of receptor binding in both stable fibroblast lines, stimulation with 5-HT mobilized significantly more intracellular Ca^{2+} in the 5-HT$_{2A}$-S314A fibroblasts when compared with wild-type 5-HT$_{2A}$ fibroblasts (110 ± 4.9% *versus* 89.8 ± 2.3% of the untreated maximal response for the 5-HT$_{2A}$-S314A and wild-type 5-HT$_{2A}$ receptors, respectively; $p < 0.05$, $n = 4$; Fig. 8*C*). These results are identical to our observations in the untreated polyclonal stable lines and suggest that a difference in receptor expression between cell lines fails to account for the apparent RSK2 insensitivity of the phosphorylation-deficient 5-HT$_{2A}$-S314A receptor. Another possibility is that changes in surface receptor expression because of altered RSK2 regulation account for the 5-HT$_{2A}$-S314A signaling phenotype. Our previous surface biotinylation data from RSK2$^{+/+}$ and RSK2$^{-/-}$ fibroblasts demonstrated that significant alterations in surface receptor expression do not occur (21). Taken together, these functional studies demonstrate that removing the Ser-314 phosphorylation site within the 5-HT$_{2A}$ receptor i3 loop renders it resistant to negative regulation by RSK2. Moreover, the potentiated signaling observed with the phosphoryla-

tion-deficient 5-HT$_{2A}$-S314A receptor is remarkably similar to what we observed in RSK2$^{-/-}$ fibroblasts and demonstrates that the 5-HT$_{2A}$-S314A receptor truly is RSK2-insensitive.

RSK2 Is Required for EGF-mediated Heterologous Desensitization of the 5-HT$_{2A}$ Receptor—Recent studies suggest that considerable bi-directional cross-talk occurs between GPCRs and RTKs. In fact, several studies support a newly emerging regulatory model whereby RTKs modulate GPCR signaling (50, 51). Our data clearly show that RSK2-mediated phosphorylation of the 5-HT$_{2A}$ receptor leads to decreased agonist responsiveness (Fig. 8). Moreover, the $^{32}P_i$ metabolic labeling data in intact fibroblasts show that EGF-activated RSK2 phosphorylates the 5-HT$_{2A}$ receptor (Fig. 7*D*). Thus it seemed plausible that EGF pretreatment could decrease 5-HT$_{2A}$ receptor responsiveness. To test this possibility, as well as to determine to what extent RSK2 is involved, we treated serum-starved RSK2$^{+/+}$ and RSK2$^{-/-}$ fibroblasts with 100 ng/ml EGF and assessed 5-HT-induced Ca^{2+} release. As shown in Fig. 9*A*, 100 ng/ml EGF activated RSK2. Interestingly, pretreatment with EGF decreased 5-HT-induced Ca^{2+} release in RSK2$^{+/+}$ fibroblasts, reaching a maximum effect at 1 h (Fig. 9*B*). Consistent with our hypothesis that EGF-activated RSK2 phosphorylates the 5-HT$_{2A}$ receptor to decrease receptor responsiveness, 1 h of EGF pretreatment failed to desensitize 5-HT$_{2A}$ signaling in RSK2$^{-/-}$ fibroblasts (Fig. 9*C*). Furthermore, the lack of desensitization in RSK2$^{-/-}$ fibroblasts demonstrates that the effects seen in RSK2$^{+/+}$ fibroblasts are not artifacts of prolonged serum starvation or EGF treatment. These results show for the first time that a growth factor can heterologously desensitize 5-HT$_{2A}$ signaling. Intriguingly, these preliminary data show that cross-talk between an RTK and the 5-HT$_{2A}$ receptor requires RSK2, and this finding may provide insight into the physiological regulation of 5-HT$_{2A}$ receptors.

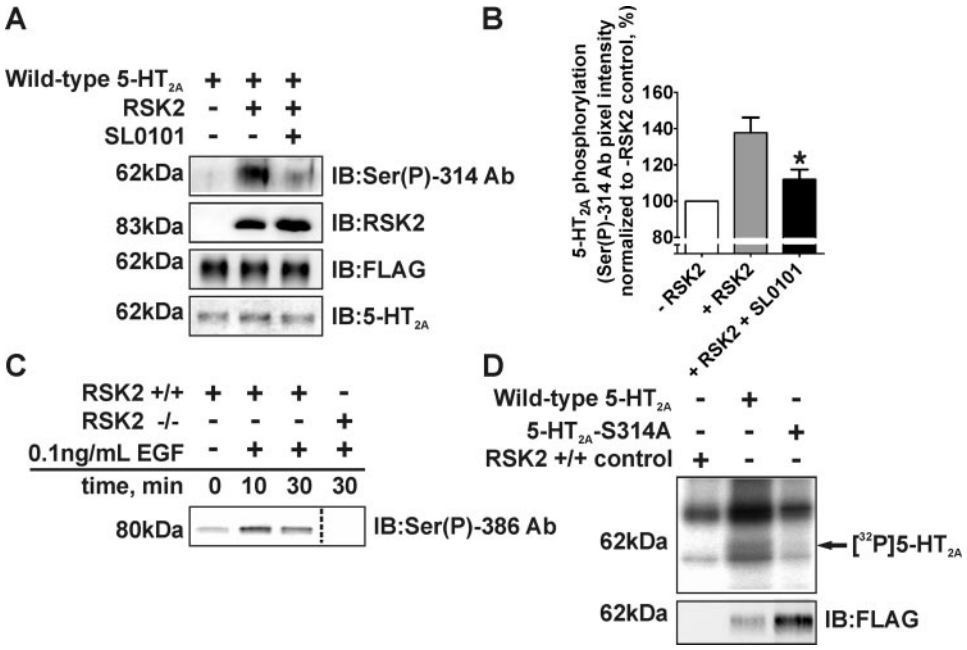

FIGURE 7. **Validation of Ser-314 phosphorylation in 5-HT$_{2A}$ receptors *in vitro* and in fibroblasts.** For these experiments purified FLAG-His$_6$ 5-HT$_{2A}$ receptors were phosphorylated *in vitro* using purified, activated RSK2 and immunoblotted (*IB*) for phospho-Ser-314 (*A* and *B*). $^{32}P_i$-Labeled RSK2$^{+/+}$ fibroblasts were treated with 0.1 ng/ml EGF for various time points and assayed for RSK2 activation (*C*) and 5-HT$_{2A}$ phosphorylation (*D*). *A,* Western blot analysis using the phospho-Ser-314-specific antibody (Ser(P)-314 Ab) verified that activated RSK2 phosphorylates Ser-314 within the 5-HT$_{2A}$ receptor i3 loop *in vitro* (*top panel*, *arrow* at ~62 kDa). The specific RSK inhibitor SL0101 (10 μM) attenuated Ser(P)-314 Ab immunolabeling. Western blot analysis of the samples loaded for Ser(P)-314 Ab detection confirmed the components of each *in vitro* kinase assay (*lower panels*). *B,* quantification of 5-HT$_{2A}$ receptor phosphorylation shown in *A*. The sum pixel intensity values (*top panel, A*) were normalized to the control assay lacking RSK2 (set to 100%). SL0101 significantly inhibited Ser(P)-314 Ab detection when compared with the *in vitro* kinase assay without SL0101. Shown here are results from five independent experiments; *, $p < 0.05$. *C,* immunoblots of purified RSK2 were probed with an antibody specific for activated RSK2 (Ser(P)-386) to show that RSK2 was activated following EGF treatment. RSK2 activation was absent in RSK2$^{-/-}$ fibroblasts. *D,* wild-type and phosphorylation-deficient 5-HT$_{2A}$-S314A receptors were immunopurified from RSK2$^{+/+}$ fibroblasts labeled with $^{32}P_i$ as stated under "Experimental Procedures." 5-HT$_{2A}$ receptors were not immunopurified from control fibroblasts lacking the FLAG-tagged 5-HT$_{2A}$ receptor. Activation of RSK2 with 0.1 ng/ml EGF resulted in increased [^{32}P]phosphate incorporation into wild-type 5-HT$_{2A}$, but not 5-HT$_{2A}$-S314A receptors (*top panel*, *arrow* ~62 kDa), suggesting that Ser-314 is phosphorylated in whole cells. Receptor purifications differed between fibroblast lines (*bottom panel*) and were normalized for autoradiography.

TABLE 2

Differences in agonist-mediated signaling between wild-type 5-HT$_{2A}$ and phosphorylation-deficient 5-HT$_{2A}$-S314A receptors in RSK2$^{+/+}$ fibroblasts

Cell line/agonist	Ca^{2+}		IP	
	Agonist potency[a] EC_{50} (pEC_{50} ± S.E.[b])	Relative agonist efficacy, %[c] E_{max} ± S.E.	Agonist potency[a] EC_{50} (pEC_{50} ± S.E.[b])	Relative agonist efficacy, %[c] E_{max} ± S.E.
Wild-type/5-HT	18.2 nM (7.74 ± 0.10)	98.7 ± 3.7	176 nM (6.76 ± 0.04)	99.6 ± 2.0
Wild-type/DOI	8.27 nM (8.08 ± 0.26)	61.5 ± 5.6	15.4 nM (7.81 ± 0.07)	63.3 ± 1.6
Wild-type/αMe5-HT	29.5 nM (7.53 ± 0.11)	95.3 ± 4.1	223 (6.65 ± 0.05)	97.1 ± 2.4
S314A/5-HT	3.83 nM (8.42 ± 0.08[d])	142 ± 3[d]	75.8 nM (7.12 ± 0.11[d])	150 ± 7[d]
S314A/DOI	2.95 nM (8.53 ± 0.12[d])	130 ± 5[d]	6.78 nM (8.17 ± 0.16[d])	126 ± 7[d]
S314A/αMe5-HT	6.24 nM (8.21 ± 0.07[d])	140 ± 4[d]	94.2 nM (7.03 ± 0.10[d])	143 ± 6[d]

[a] Agonist potencies (EC_{50}) and efficacies (E_{max}) were determined for agonist-mediated Ca^{2+} release and IP accumulation. The results represent the average of three independent experiments.
[b] pEC_{50} values are represented as −log of EC_{50} in molar.
[c] For each experiment the maximum response to 5-HT in fibroblasts expressing wild-type 5-HT$_{2A}$ receptors was set equal to 100%.
[d] For each agonist the value was statistically different from fibroblasts expressing wild-type 5-HT$_{2A}$ receptors, $p < 0.05$.

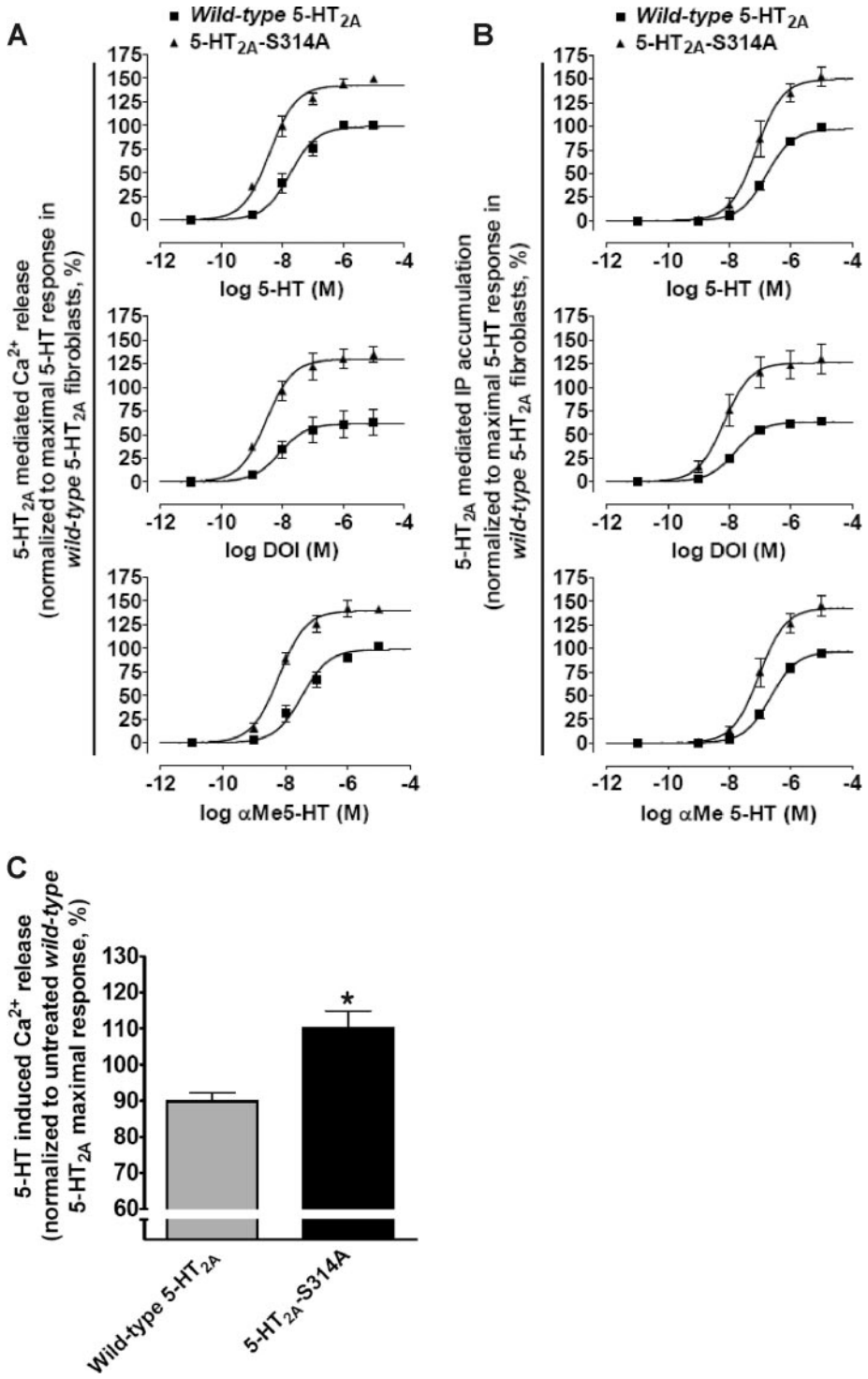

FIGURE 8. **Regulation by RSK2 requires Ser-314 phosphorylation within the 5-HT$_{2A}$ receptor i3 loop.** RSK2$^{+/+}$ fibroblasts stably expressing either the wild-type 5-HT$_{2A}$ or phosphorylation-deficient 5-HT$_{2A}$-S314A receptors were treated with 5-HT$_{2A}$ agonists and increases in intracellular Ca^{2+} (*A*) and inositol phosphates (*IP*) (*B*) were measured. Wild-type and 5-HT$_{2A}$-S314A receptor signaling were also examined after normalizing receptor expression with EEDQ (*C*) as outlined under "Experimental Procedures." *A,* FLIPR analysis using a calcium-sensitive dye shows that 5-HT, DOI, and α-Me5-HT elicited significantly greater increases in intracellular Ca^{2+} in 5-HT$_{2A}$-S314A fibroblasts relative to wild-type 5-HT$_{2A}$-expressing fibroblasts. The base-line subtracted RFU values were normalized to cell number and maximal wild-type 5-HT response (set to 100%). Shown here are results from three independent experiments in which all measures of relative efficacy (E_{max}) and potency (EC_{50}) were significant, $p < 0.05$. *B*, scintillation proximity assays show that 5-HT, DOI, and α-Me5-HT elicited significantly greater increases in [^{3}H]inositol phosphates in 5-HT$_{2A}$-S314A fibroblasts relative to wild-type 5-HT$_{2A}$-expressing fibroblasts. The base-line subtracted counts/min values were normalized to cell number and maximal wild-type 5-HT response (set to 100%). Shown here are the results from three independent experiments in which all measures of relative efficacy (E_{max}) and potency (EC_{50}) were significant, $p < 0.05$. *C,* under conditions of equal receptor expression, 5-HT$_{2A}$-S314A fibroblasts released more intracellular Ca^{2+} than wild-type 5-HT$_{2A}$-expressing fibroblasts. Shown here are normalized relative efficacy values (maximal untreated wild-type 5-HT response set to 100% as in *A*) from four independent experiments in which EEDQ treatments produced similar levels of specific [^{3}H]ketanserin binding; *, $p < 0.05$.

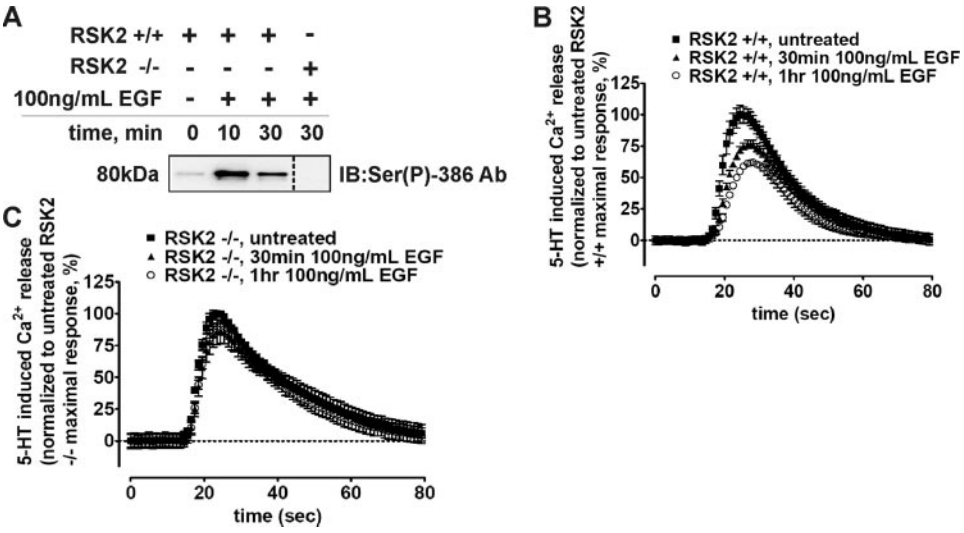

FIGURE 9. **RSK2 is necessary for EGF-mediated desensitization of 5-HT$_{2A}$ receptors.** RSK2$^{+/+}$ and RSK2$^{-/-}$ fibroblasts stably expressing wild-type 5-HT$_{2A}$ receptors were treated with 100 ng/ml EGF for various time points, and RSK2 activation (*A*) and 5-HT-mediated (10 nM) intracellular Ca^{2+} release in RSK2$^{+/+}$ (*B*) and RSK2$^{-/-}$ (*C*) fibroblasts was determined. *A,* immunoblots of purified RSK2 were probed with an antibody specific for activated RSK2 (Ser(P)-386) to show that RSK2 was robustly activated following EGF treatment. RSK2 activation was absent in RSK2$^{-/-}$ fibroblasts. *B,* FLIPR analysis of Ca^{2+} release in EGF-pretreated RSK2$^{+/+}$ fibroblasts (▲, ○) identified a time-dependent decrease in 5-HT$_{2A}$ responsiveness when compared with untreated fibroblasts (■). EGF-mediated heterologous desensitization was maximal at 1 h (○) and was observed in three independent experiments. Shown are normalized traces from a single experiment. *C,* FLIPR analysis of Ca^{2+} release in EGF-pretreated RSK2$^{-/-}$ fibroblasts showed no effect of EGF when compared with untreated fibroblasts. This result was observed in three independent experiments, and shown here are normalized traces from a single experiment.

DISCUSSION

This paper has three major findings. First, we demonstrate via multiple lines of evidence that RSK2, a downstream effector of ERK that interacts with and negatively regulates 5-HT$_{2A}$ receptor signaling in fibroblasts (21), exerts its novel regulatory effect on 5-HT$_{2A}$ activity by phosphorylating the i3 loop at the conserved Ser-314. This result is important because it is the first successful demonstration of a *bona fide* 5-HT$_{2A}$ receptor phosphorylation site, and because it is the first evidence that a downstream member of the ERK/MAPK pathway phosphorylates a GPCR. Additionally, we correlate receptor phosphorylation at Ser-314 with altered receptor activity. Second, our findings suggest for the first time that Ser-314, and possibly other conserved residues situated in the C-terminal portion of the i3 loop, plays a critical role in determining 5-HT$_{2A}$ receptor activity. Third, we provide the first evidence demonstrating growth factor-mediated heterologous desensitization of 5-HT$_{2A}$ receptors, a novel regulatory paradigm that requires RSK2.

RSK2 Phosphorylates the 5-HT$_{2A}$ Receptor i3 Loop at Ser-314—Protein phosphorylation, in general, is an indispensable post-translational regulatory mechanism mediated by protein kinases and exploited by the cell to modulate protein signaling cascades, enzyme catalysis, and protein-protein interactions. For GPCRs, protein kinases induce GPCR desensitization via a process in which distinct intracellular residues are phosphorylated, thereby uncoupling the receptor from its cognate G protein (52). For more than 20 years it has been appreciated that various kinases can regulate 5-HT$_{2A}$ signaling (12, 53), and although it is clear that PKC plays an important role in modulating 5-HT$_{2A}$ receptor signaling, it is unclear if PKC or any other kinase directly phosphorylates the 5-HT$_{2A}$ receptor. A recent study by Turner *et al.* (54) using purified PKC and a peptide corresponding to amino acids 377–396 of the human 5-HT$_{2A}$ receptor C terminus provided the first direct biochemical evidence that PKC can phosphorylate a 5-HT$_{2A}$-derived peptide *in vitro*. Moreover, PKC-mediated phosphorylation of the peptide was inhibited by calmodulin thereby providing an intriguing regulatory scenario (18). A previous study by Vouret-Craviari *et al.* (55) identified basal but not agonist-induced phosphorylation of the 5-HT$_{2A}$ receptor in HEK293 cells, although the identity of the kinase was not determined. Despite the ability of PKC, and most likely other kinases, to modulate 5-HT$_{2A}$ signaling, it was still unclear, until now, whether 1) the full-length 5-HT$_{2A}$ receptor is phosphorylated by a specific kinase(s) and 2) if 5-HT$_{2A}$ receptor phosphorylation itself modulates receptor signaling.

It is clear from our previous work that RSK2 negatively regulates 5-HT$_{2A}$ signaling, as evidenced by augmented transient Ca^{2+} release and IP accumulation in RSK2$^{-/-}$ fibroblasts (21). Here we provide supporting time course data that show that both rapid and prolonged 5-HT$_{2A}$ signaling events are dysregulated in RSK2$^{-/-}$ fibroblasts. Close examination of our previous results suggested to us that RSK2 most likely negatively regulates 5-HT$_{2A}$ receptor function proximal to receptor activation by directly phosphorylating the receptor i3 loop. Specifically, our decision to focus on receptor phosphorylation was influenced by the following two major observations: 1) previous evidence indicated that RSK2 interacts with the 5-HT$_{2A}$ receptor i3 loop within a highly conserved region containing the RSK2-like phosphorylation motif ^{275}RAKLAS^{280} (21, 23), and 2) extensive control experiments suggested that signaling components downstream from the receptor are unaltered (21).

In the approach outlined here we incorporated a variety of techniques designed to dissect and unequivocally determine whether RSK2 modulates 5-HT$_{2A}$ function via direct receptor phosphorylation. The data presented here progressed from the following: 1) initial experiments that demonstrated that RSK2 kinase activity is essential for attenuating 5-HT$_{2A}$ signaling and promoting 5-HT$_{2A}$ receptor phosphorylation (*i.e.* kinase-dead rescue assays and *in vitro* kinase assays); 2) to experiments that identified and validated the novel Ser-314 phosphorylation site (*i.e.* tandem MS, site-directed mutagenesis, phospho-specific immunoblotting, and metabolic labeling assays); 3) to functional experiments that determined that removal of the phos-

pho-acceptor site (S314A) compromises the ability of RSK2 to negatively regulate 5-HT$_{2A}$ signaling (*i.e.* intracellular Ca^{2+} release and IP accumulation assays); and 4) to functional experiments that determined that EGF desensitizes 5-HT$_{2A}$ signaling through RSK2. In this approach we used a broad spectrum of standard techniques such as MS and $^{32}P_i$ metabolic labeling that have been invaluable for the discovery of GPCR phosphorylation sites (43–47, 56–59).

One particularly surprising result of our study was that the unbiased MS experiments failed to identify Ser-280 as a major site of RSK2 phosphorylation in both the i3 peptide and full-length receptor. We initially predicted that RSK2 would phosphorylate Ser-280 located within the RSK2-like consensus phosphorylation motif ^{275}RAKLAS^{280}, a region of the i3 loop that is highly conserved among rat, human, and mouse 5-HT$_{2A}$ receptors. Our inability to demonstrate that RSK2 targets Ser-280 within the consensus phosphorylation motif was independently verified in the i3 loop peptide using both site-directed mutagenesis and phospho-specific immunoblotting strategies. Evidence showing that the highly conserved RSK2-like ^{275}RAKLAS^{280} phosphorylation motif did not contribute to receptor phosphorylation suggests that the motif may have additional functions. For example, it is likely that this region targets RSK2 to the 5-HT$_{2A}$ receptor, because yeast two-hybrid experiments showed that this region of the i3 loop facilitates RSK2 binding (21). Several low abundance phosphopeptides were also identified, but similar to Ser-280, site-directed mutagenesis studies showed that these sites failed to influence overall phosphorylation levels. Moreover, almost complete loss of $^{32}P_i$ incorporation into the phosphorylation-deficient 5-HT$_{2A}$-S314A receptor in our metabolic labeling study suggested that few, if any, additional RSK2 phosphorylation sites exist. These results strongly suggest that RSK2 favors Ser-314 phosphorylation *in vitro* and in intact cells.

Ser-314 Is Positioned to Modulate 5-HT$_{2A}$ Signaling—Our finding that RSK2 phosphorylation within a conserved region of the i3 loop has functional consequences is consistent with several studies by our lab and others suggesting that the i3 loop is important for directing and promoting GPCR signaling. Specifically, we demonstrated that the purified 5-HT$_{2A}$ receptor i3 loop is predominantly α-helical and binds purified arrestins (29). Previous work also suggests that peptides corresponding to C-terminal regions of the 5-HT$_{2A}$ i3 loop directly interact with and activate purified Gα_q (2). These findings agree with several studies suggesting that amphipathic α-helices are involved in determining receptor-G protein binding (60, 61) and may, in fact, be intrinsic to Gα_q coupling as suggested by the recent structure of Gα_q-coupled squid rhodopsin (62). Furthermore, merely introducing the i3 loop of the Gα_q-coupled 5-HT$_{2A}$ receptor into the Gα_i-coupled 5-HT$_{1B}$ receptor (5-HT$_{1B/2A}$) is sufficient to shift its coupling specificity from inhibition of adenylyl cyclase to phospholipase C activation (63). Together with previous studies showing that introduction of phosphorylated residues into the cytoplasmic domains of many GPCRs inhibits signaling, it seems likely that Ser-314 phosphorylation functionally uncouples the 5-HT$_{2A}$ receptor from its cognate G protein.

An additional mechanism by which Ser-314 phosphorylation (here denoted as 6.26 (64), Fig. 6*B, arrow*) modulates 5-HT$_{2A}$ receptor function could be related to its close proximity to a highly conserved salt bridge between Glu-318 on transmembrane helix VI (E318, denoted 6.30, *arrow* Fig. 6*B*) and an Arg residue (denoted 3.50) located in a highly conserved stretch of amino acids ((D/E)RY) located at the interface between transmembrane III and the second intracellular loop (65). This intramolecular salt bridge interaction is thought to play a pivotal role in regulating GPCR conformational states because it is retained in the ground state structure of rhodopsin and disrupted in the constitutively active β_2-adrenergic receptor (66, 67). Specifically, homology modeling of the 5-HT$_{2A}$ receptor based on rhodopsin places Ser-314 (6.26) one helical turn down from Glu-318 (6.30), and studies from our lab show that disrupting this "ionic lock" by mutating Glu-318(6.30) to Arg increases constitutive activity and agonist affinity of the 5-HT$_{2A}$ receptor (68). With regard to our data it remains a possibility that the converse situation also occurs; phosphorylation of Ser-314(6.26) one helical turn down from Glu-318(6.30) promotes stability of the ionic lock, thus favoring the inactive receptor conformation. In fact, preliminary evidence suggests that either of these scenarios is plausible because mutating Ser-314 to Asp (phosphomimetic) in the 5-HT$_{2A}$ receptor attenuates agonist-induced IP accumulation.[3] Nonetheless, the mechanism explaining how Ser-314(6.26) phosphorylation negatively regulates 5-HT$_{2A}$ receptor function is fascinating and will be the subject of intense future investigation.

Components of MAPK and RTK Pathways Modulate 5-HT$_{2A}$ Signaling—Most importantly, these findings are the first to conclusively demonstrate that a downstream MAPK/ERK cascade signaling protein interacts with and directly phosphorylates a GPCR, thereby modulating its signaling capacity. It has become increasingly clear that GPCR signaling through an entirely G protein-mediated pathway fails to account for the diversity of responses resulting from GPCR activation (69), especially the effects on cell growth and differentiation. It is now realized that these responses are mediated by complex GPCR signaling networks converging upon the activation of MAPKs (70). GPCRs are thought to transactivate the MAPK cascade through numerous effectors, including activation of EGF, platelet-derived growth factor, fibroblast growth factor, and neurotrophin RTKs. GPCRs transactivate RTKs through several routes, including a ligand-dependent process utilizing ADAM family metalloproteinases resulting in subsequent ectodomain shedding of RTK ligands, as well as ligand-independent processes, including activation of tyrosine kinases and production of reactive oxygen species. 5-HT$_{2A}$ agonists are well known to activate ERK, and we have reported that agonist stimulation of 5-HT$_{2A}$ receptors results in a time-dependent increase in ERK1/2 activation in fibroblasts (21). In fact, recent studies have identified several signaling intermediates linking the 5-HT$_{2A}$ receptor to ERK/MAPK transactivation. Greene *et al.* (71) reported that 5-HT$_{2A}$ receptors in rat renal mesangial

[3] J. A. Gray and B. L. Roth, unpublished observations.

cells transactivate ERK via H_2O_2 generation. Specifically, phospholipase C, PKC, and reactive oxygen species generated by a NAD(P)H oxidase enzyme were implicated in the activation of ERK. An additional study in renal mesangial cells found that tumor necrosis factor α-converting enzyme (TACE, ADAM17) was responsible for 5-HT$_{2A}$-mediated, ligand-induced transactivation of the EGF receptor and ultimately activation of ERK (72). It is clear that 5-HT$_{2A}$ receptors transactivate the MAPK/ERK cascade; therefore, our results are consistent with the intriguing possibility that RSK2 is activated downstream of ERK, thereby exerting negative feedback control on 5-HT$_{2A}$ signaling (*i.e.* homologous desensitization). Importantly, our metabolic labeling experiments did not detect 5-HT$_{2A}$ phosphorylation under basal conditions or following stimulation with 5-HT,[4] which is in agreement with others (55). It remains a possibility that our methods are not sensitive enough to detect low levels of receptor phosphorylation; therefore, we are actively pursuing additional studies to determine whether RSK2 plays an important role in mediating homologous desensitization of the 5-HT$_{2A}$ receptor.

Adding to the growing complexity of GPCR signaling are studies suggesting that RTKs return the favor and modulate GPCR function (73). For instance, several groups have established that RTK activation modulates GPCR signaling (*e.g.* β_1-adrenergic receptor, β_2-adrenergic receptor, and α_1-adrenergic receptors) (50, 51). Here we report for the first time that activation of RSK2 by the RTK agonist EGF leads to phosphorylation of 5-HT$_{2A}$ receptors in intact cells. Furthermore, we report the novel finding that EGF pretreatment time-dependently desensitizes 5-HT$_{2A}$ signaling in mouse embryonic fibroblasts, a result that requires RSK2. As discussed above, our current observations do not support RSK2-mediated homologous desensitization of the 5-HT$_{2A}$ receptor. On the other hand, our data are consistent with a heterologous desensitization model in which growth factors activate RTKs and downstream MAPKs, which in turn activate RSK2 and phosphorylate the 5-HT$_{2A}$ receptor to modulate its function. Notably, this finding may have far-reaching implications for human diseases associated with 5-HT$_{2A}$ dysregulation because some RTKs are considered susceptibility factors for several psychiatric diseases (74).

In summary, multiple lines of evidence support the hypothesis that activated RSK2 regulates 5-HT$_{2A}$ receptor function by directly phosphorylating the 5-HT$_{2A}$ receptor. This study presents the first evidence that phosphorylation of the 5-HT$_{2A}$ receptor at Ser-314, which is located within a highly conserved region of the i3 loop, modulates its function. Previous studies suggest that a phosphorylation event at Ser-314 is likely to affect receptor signaling because its location in the i3 loop is associated with G protein coupling as well as the regulation of GPCR conformational states. These findings further support a novel regulatory mechanism whereby RSK2, a downstream effector of the ERK/MAPK cascade, directly interacts with and phosphorylates a GPCR as well as mediates cross-talk between a growth factor and a GPCR.

[4] B. L. Roth, unpublished observations.

REFERENCES

1. de Clerck, F., David, J. L., and Janssen, P. A. (1982) *Agents Actions* **12,** 388–397
2. Roth, B. L., Willins, D. L., Kristiansen, K., and Kroeze, W. K. (1998) *Pharmacol. Ther.* **79,** 231–257
3. Williams, G. V., Rao, S. G., and Goldman-Rakic, P. S. (2002) *J. Neurosci.* **22,** 2843–2854
4. Aghajanian, G. K., and Marek, G. J. (1997) *Neuropharmacology* **36,** 589–599
5. Nichols, D. E. (2004) *Pharmacol. Ther.* **101,** 131–181
6. Roth, B. L., Baner, K., Westkaemper, R., Siebert, D., Rice, K. C., Steinberg, S., Ernsberger, P., and Rothman, R. B. (2002) *Proc. Natl. Acad. Sci. U. S. A.* **99,** 11934–11939
7. Roth, B. L. (1994) *Ann. Clin. Psychiatry* **6,** 67–78
8. Kroeze, W. K., Sheffler, D. J., and Roth, B. L. (2003) *J. Cell Sci.* **116,** 4867–4869
9. Krupnick, J. G., and Benovic, J. L. (1998) *Annu. Rev. Pharmacol. Toxicol.* **38,** 289–319
10. Kelly, E., Bailey, C. P., and Henderson, G. (2008) *Br. J. Pharmacol.* **153,** Suppl. 1, 379–388
11. Tobin, A. B. (2008) *Br. J. Pharmacol.* **153,** Suppl. 1, 167–176
12. Roth, B. L., Nakaki, T., Chuang, D. M., and Costa, E. (1986) *J. Pharmacol. Exp. Ther.* **238,** 480–485
13. Rahimian, R., and Hrdina, P. D. (1995) *Can. J. Physiol. Pharmacol.* **73,** 1686–1691
14. Rahman, S., McLean, J. H., Darby-King, A., Paterno, G., Reynolds, J. N., and Neuman, R. S. (1995) *Neuroscience* **66,** 891–901
15. Marek, G. J., and Aghajanian, G. K. (1995) *Synapse* **21,** 123–130
16. Kagaya, A., Mikuni, M., Kusumi, I., Yamamoto, H., and Takahashi, K. (1990) *J. Pharmacol. Exp. Ther.* **255,** 305–311
17. Roth, B. L., Palvimaki, E. P., Berry, S., Khan, N., Sachs, N., Uluer, A., and Choudhary, M. S. (1995) *J. Pharmacol. Exp. Ther.* **275,** 1638–1646
18. Berg, K. A., Stout, B. D., Maayani, S., and Clarke, W. P. (2001) *J. Pharmacol. Exp. Ther.* **299,** 593–602
19. Hanley, N. R., and Hensler, J. G. (2002) *J. Pharmacol. Exp. Ther.* **300,** 468–477
20. Gray, J. A., Sheffler, D. J., Bhatnagar, A., Woods, J. A., Hufeisen, S. J., Benovic, J. L., and Roth, B. L. (2001) *Mol. Pharmacol.* **60,** 1020–1030
21. Sheffler, D. J., Kroeze, W. K., Garcia, B. G., Deutch, A. Y., Hufeisen, S. J., Leahy, P., Bruning, J. C., and Roth, B. L. (2006) *Proc. Natl. Acad. Sci. U. S. A.* **103,** 4717–4722
22. Frodin, M., and Gammeltoft, S. (1999) *Mol. Cell. Endocrinol.* **151,** 65–77
23. Leighton, I. A., Dalby, K. N., Caudwell, F. B., Cohen, P. T., and Cohen, P. (1995) *FEBS Lett.* **375,** 289–293
24. Hanauer, A., and Young, I. D. (2002) *J. Med. Genet.* **39,** 705–713
25. Bruning, J. C., Gillette, J. A., Zhao, Y., Bjorbaeck, C., Kotzka, J., Knebel, B., Avci, H., Hanstein, B., Lingohr, P., Moller, D. E., Krone, W., Kahn, C. R., and Muller-Wieland, D. (2000) *Proc. Natl. Acad. Sci. U. S. A.* **97,** 2462–2467
26. Zhao, Y., Bjorbaek, C., and Moller, D. E. (1996) *J. Biol. Chem.* **271,** 29773–29779
27. Morgenstern, J. P., and Land, H. (1990) *Nucleic Acids Res.* **18,** 1068
28. Xia, Z., Gray, J. A., Compton-Toth, B. A., and Roth, B. L. (2003) *J. Biol. Chem.* **278,** 21901–21908
29. Gelber, E. I., Kroeze, W. K., Willins, D. L., Gray, J. A., Sinar, C. A., Hyde, E. G., Gurevich, V., Benovic, J., and Roth, B. L. (1999) *J. Neurochem.* **72,** 2206–2214
30. Bradford, M. M. (1976) *Anal. Biochem.* **72,** 248–254
31. Munson, P. J., and Rodbard, D. (1980) *Anal. Biochem.* **107,** 220–239
32. Cohen, M. S., Zhang, C., Shokat, K. M., and Taunton, J. (2005) *Science* **308,** 1318–1321
33. Backstrom, J. R., and Sanders-Bush, E. (1997) *J. Neurosci. Methods* **77,** 109–117
34. Gray, J. A., Compton-Toth, B. A., and Roth, B. L. (2003) *Biochemistry* **42,** 10853–10862
35. Bourdon, D. M., Wing, M. R., Edwards, E. B., Sondek, J., and Harden, T. K. (2006) *Methods Enzymol.* **406,** 489–499

36. Fisher, T. L., and Blenis, J. (1996) *Mol. Cell. Biol.* **16,** 1212–1219
37. Poteet-Smith, C. E., Smith, J. A., Lannigan, D. A., Freed, T. A., and Sturgill, T. W. (1999) *J. Biol. Chem.* **274,** 22135–22138
38. Hanlon, M., Sturgill, T. W., and Sealy, L. (2001) *J. Biol. Chem.* **276,** 38449–38456
39. Chrestensen, C. A., and Sturgill, T. W. (2002) *J. Biol. Chem.* **277,** 27733–27741
40. Sturgill, T. W., Ray, L. B., Erikson, E., and Maller, J. L. (1988) *Nature* **334,** 715–718
41. Smith, J. A., Poteet-Smith, C. E., Xu, Y., Errington, T. M., Hecht, S. M., and Lannigan, D. A. (2005) *Cancer Res.* **65,** 1027–1034
42. Sapkota, G. P., Cummings, L., Newell, F. S., Armstrong, C., Bain, J., Frodin, M., Grauert, M., Hoffmann, M., Schnapp, G., Steegmaier, M., Cohen, P., and Alessi, D. R. (2007) *Biochem. J.* **401,** 29–38
43. January, B., Seibold, A., Whaley, B., Hipkin, R. W., Lin, D., Schonbrunn, A., Barber, R., and Clark, R. B. (1997) *J. Biol. Chem.* **272,** 23871–23879
44. Bouvier, M., Hausdorff, W. P., De Blasi, A., O'Dowd, B. F., Kobilka, B. K., Caron, M. G., and Lefkowitz, R. J. (1988) *Nature* **333,** 370–373
45. Sibley, D. R., Strasser, R. H., Benovic, J. L., Daniel, K., and Lefkowitz, R. J. (1986) *Proc. Natl. Acad. Sci. U. S. A.* **83,** 9408–9412
46. El Kouhen, R., Burd, A. L., Erickson-Herbrandson, L. J., Chang, C. Y., Law, P. Y., and Loh, H. H. (2001) *J. Biol. Chem.* **276,** 12774–12780
47. Kouhen, O. M., Wang, G., Solberg, J., Erickson, L. J., Law, P. Y., and Loh, H. H. (2000) *J. Biol. Chem.* **275,** 36659–36664
48. Xing, J., Ginty, D. D., and Greenberg, M. E. (1996) *Science* **273,** 959–963
49. Kang, S., Dong, S., Guo, A., Ruan, H., Lonial, S., Khoury, H. J., Gu, T. L., and Chen, J. (2008) *J. Biol. Chem.* **283,** 4652–4657
50. Gavi, S., Shumay, E., Wang, H. Y., and Malbon, C. C. (2006) *Trends Endocrinol. Metab.* **17,** 48–54
51. Gavi, S., Yin, D., Shumay, E., Wang, H. Y., and Malbon, C. C. (2007) *Endocrinology* **148,** 2653–2662
52. Ferguson, S. S., Barak, L. S., Zhang, J., and Caron, M. G. (1996) *Can. J. Physiol. Pharmacol.* **74,** 1095–1110
53. Allen, J. A., Yadav, P. N., and Roth, B. L. (2008) *Neuropharmacology* **55,** 961–968
54. Turner, J. H., Gelasco, A. K., and Raymond, J. R. (2004) *J. Biol. Chem.* **279,** 17027–17037
55. Vouret-Craviari, V., Auberger, P., Pouyssegur, J., and Van Obberghen-Schilling, E. (1995) *J. Biol. Chem.* **270,** 4813–4821
56. Karoor, V., and Malbon, C. C. (1996) *J. Biol. Chem.* **271,** 29347–29352
57. Ohguro, H., Palczewski, K., Ericsson, L. H., Walsh, K. A., and Johnson, R. S. (1993) *Biochemistry* **32,** 5718–5724
58. Ohguro, H., Van Hooser, J. P., Milam, A. H., and Palczewski, K. (1995) *J. Biol. Chem.* **270,** 14259–14262
59. Soskic, V., Nyakatura, E., Roos, M., Muller-Esterl, W., and Godovac-Zimmermann, J. (1999) *J. Biol. Chem.* **274,** 8539–8545
60. Hamm, H. E., Deretic, D., Arendt, A., Hargrave, P. A., Koenig, B., and Hofmann, K. P. (1988) *Science* **241,** 832–835
61. Duerson, K., Carroll, R., and Clapham, D. (1993) *FEBS Lett.* **324,** 103–108
62. Murakami, M., and Kouyama, T. (2008) *Nature* **453,** 363–367
63. Oksenberg, D., Havlik, S., Peroutka, S. J., and Ashkenazi, A. (1995) *J. Neurochem.* **64,** 1440–1447
64. Ballesteros, J. A., and Weinstein, H. (1995) *Methods Neurosci.* **25,** 366–428
65. Rovati, G. E., Capra, V., and Neubig, R. R. (2007) *Mol. Pharmacol.* **71,** 959–964
66. Palczewski, K., Kumasaka, T., Hori, T., Behnke, C. A., Motoshima, H., Fox, B. A., Le Trong, I., Teller, D. C., Okada, T., Stenkamp, R. E., Yamamoto, M., and Miyano, M. (2000) *Science* **289,** 739–745
67. Rasmussen, S. G., Choi, H. J., Rosenbaum, D. M., Kobilka, T. S., Thian, F. S., Edwards, P. C., Burghammer, M., Ratnala, V. R., Sanishvili, R., Fischetti, R. F., Schertler, G. F., Weis, W. I., and Kobilka, B. K. (2007) *Nature* **450,** 383–387
68. Shapiro, D. A., Kristiansen, K., Weiner, D. M., Kroeze, W. K., and Roth, B. L. (2002) *J. Biol. Chem.* **277,** 11441–11449
69. Urban, J. D., Clarke, W. P., von Zastrow, M., Nichols, D. E., Kobilka, B., Weinstein, H., Javitch, J. A., Roth, B. L., Christopoulos, A., Sexton, P. M., Miller, K. J., Spedding, M., and Mailman, R. B. (2007) *J. Pharmacol. Exp. Ther.* **320,** 1–13
70. Pierce, K. L., Luttrell, L. M., and Lefkowitz, R. J. (2001) *Oncogene* **20,** 1532–1539
71. Greene, E. L., Houghton, O., Collinsworth, G., Garnovskaya, M. N., Nagai, T., Sajjad, T., Bheemanathini, V., Grewal, J. S., Paul, R. V., and Raymond, J. R. (2000) *Am. J. Physiol.* **278,** F650–F658
72. Gooz, M., Gooz, P., Luttrell, L. M., and Raymond, J. R. (2006) *J. Biol. Chem.* **281,** 21004–21012
73. Delcourt, N., Bockaert, J., and Marin, P. (2007) *Trends Pharmacol. Sci.* **28,** 602–607
74. Mei, L., and Xiong, W. C. (2008) *Nat. Rev. Neurosci.* **9,** 437–452
75. Berger, M., Gray, J. A., and Roth, B. L. (2009) *Annu. Rev. Med.* **60,** 355–366